IDENTIFICATION AND FUNCTIONAL CHARACTERIZATION OF A LONG NON-CODING RNA ASSOCIATED WITH PROSTATE CANCER

by

MD FAQRUL HASAN
B.S. University of Dhaka, 2012
M.S. University of Dhaka, 2014

A thesis submitted in partial fulfillment of the requirements
for the degree of Master of Science
in the Burnett School of Biomedical Sciences
in the College of Medicine
at the University of Central Florida
Orlando, Florida

Spring Term
2019

ABSTRACT

Prostate cancer is the most common cancer in men in the western world. Although early stage prostate cancer is treatable late stage, more specifically, metastatic and drug resistant prostate cancers are mostly incurable. The failure of current treatments obligates the research community to explore novel areas in prostate cancer biology and find better therapeutic targets. Emerging evidences show that non-coding RNAs specifically long non-coding RNAs (lncRNAs) play regulatory roles in various cellular processes and are frequently dysregulated in cancer including prostate cancer. These aberrantly expressed lncRNAs mostly with unexplored genetic information may drive cancer progression. Previous studies done in our laboratory showed a tumor suppressor role of a cluster of small non-coding RNAs or microRNA (miRNA) miR-17-92a in PC-3 prostate cancer cells. To learn the underlying mechanism, transcriptome analysis with or without expression of miR-17-92a was conducted in our laboratory. RNA-sequencing data analysis identified reduced expression of a set of lncRNAs and oncogenes, and up regulation of several tumor suppressor genes upon expression of miR-17-92a cluster miRNAs. One of the down regulated intergenic lncRNAs, PAINT (Prostate Cancer Associated Intergenic Non-coding Transcript) (LINC00888), was selected for determining its functional role in prostate cancer. TCGA and GEO profiles analyses revealed up regulation of PAINT in prostate tumors with higher Gleason Scores, in highly aggressive metastatic prostate cancer cell lines, and upon androgen deprivation therapy of prostate cancer cells. This observation was supported by our studies on expression analysis of PAINT in prostate tumor tissues using RNA in-situ hybridization in tissue microarrays (TMA) containing tissues from different stages of prostate cancer and normal prostate tissues, which showed higher expression of PAINT in prostate cancer tissues compared to normal

tissues. Furthermore, late stage (stage III and stage IV) prostate tumors showed significant overexpression of PAINT compared to early stage (stage II) prostate cancer tissues. We examined the functional relevance of PAINT in promoting tumor progression next using different prostate cancer cell lines. Silencing of PAINT using siRNAs showed decreased cell proliferation, reduced S-phase progression and activation of pro-apoptotic proteins PARP and Caspase-3. Silencing of PAINT also showed decreased cell migration and increased expression of the epithelial marker, E-cadherin while reduced expression of mesenchymal markers Slug and Vimentin. Ectopic expression of PAINT reversed the effects observed upon silencing of PAINT. Increased cell proliferation, cell cycle progression and cell migration were noted in prostate cancer cells overexpressing PAINT. Additionally, cancer promoting phenotype such as larger colony formation and higher expression of mesenchymal marker Slug, was detected upon overexpression of PAINT. Our study also determined the therapeutic benefit of inhibition of expression showing an increased sensitivity of metastatic prostate cancer cells to the chemotherapeutic agent docetaxel (DTX) and selective Aurora kinase inhibitor VX-680. Taken together, our study establishes an oncogenic function of PAINT, its clinical relevance as a marker for advanced stage prostate cancer and its potential as a therapeutic target for metastatic prostate cancer.

ACKNOWLEDGEMENTS

First, I would like to thank Dr. Ratna Chakrabarti for her guidance and encouragement as my mentor. I would also like to acknowledge my labmates and friends for their continuous support, which gave me the strength to carry on. My heartfelt gratitude goes to Dr. Thomas Andl for his guidance and assistance during my research. Finally, I would like to thank my committee members, Dr. Jihe Zhao, Dr. Shaojie Zhang for their valuable support and guidance throughout my thesis.

TABLE OF CONTENTS

LIST OF FIGURES

LIST OF TABLES

LIST OF ABBREVIATIONS

ADT - Androgen Deprivation Therapy

AIPC - Androgen Independent Prostate Cancer

AR - Androgen Receptor

CRPC - Castration Resistant Prostate Cancer

DTX - Docetaxel (anti-mitotic chemotherapeutic)

EMT- Epithelial Mesenchymal Transition

LncRNA - long non-coding RNA

LINC00888 - Long Intergenic Non-protein Coding RNA 888

miRNA - microRNA

PAINT - Prostate Cancer Associated Intergenic Non-coding Transcript

PCa - Prostate cancer

TMA - Tissue Microarray

CHAPTER ONE: INTRODUCTION

1.1 Non-Coding RNA and Cancer

Non-coding RNAs are commonly RNA molecules that do not encode for proteins (1). Most widely known subclasses of non-coding RNAs are ribosomal RNAs (rRNAs and transfer RNAs (tRNAs). Other functionally important subclasses include long non-coding RNAs (lncRNAs), microRNAs (miRNAs), small interfering RNAs (siRNAs), piwi-interacting RNAs (piRNAs), small nucleolar RNAs (snoRNAs) and small nuclear (snRNAs) (2). In general, non-coding RNAs are mainly classified as long and small non-coding RNAs based on an arbitrary cut-off length of 200 nucleotide bases. These non- coding RNAs can be involved in essential biological processes such as DNA replication, transcriptional regulation, RNA splicing, translation, post-translational modification and maintenance of genome integrity (2). However, it has been observed that non-coding RNAs play a significant role as regulatory molecules in several diseases including cancer, and often show aberrant expression patterns which are linked to the progression of the disease stage (3) (4). Although studies are now showing the importance of non-coding RNAs in several cancer types, there is still a lack of functional characterization of most of the dysregulated non-coding RNAs and how this may potentially impact cancer progression and drug resistance. These unexplored areas of genomic science have gained huge attention because non-coding RNAs can have multiple targets and their involvement in cancer and other deadly diseases could play a major role in the advancement of diagnostic and therapeutic avenues.

1.1.1 LncRNA: Overview

Long non-coding RNAs (LncRNAs) are one of the major groups of non-coding RNAs which does not have any universal definition. The most accepted definition is that lncRNAs are long RNA molecules with no absolute protein coding potential. There are some general features of LncRNAs that make it a unique class of RNA molecules. Firstly, most lncRNAs are longer than 200 bp. However, this length based classification is an arbitrary cut-off, not a universal feature, to differentiate lncRNAs from other short non-coding RNAs. Secondly, lncRNAs are separated from protein coding RNAs due to their inability to make proteins. Recent next generation sequencing based studies revealed that some of the lncRNAs may harbor cryptic open reading frames (ORFs) (5)(6).

A large population of lncRNAs share several common characteristics with mRNA transcripts; these lncRNAs are transcribed by RNA polymerase II, contains the 5' cap, uses alternative splicing to produce mature lncRNAs and have polyadenylated tail like mRNAs (7) (8). Although there is no absolute distinction between protein coding and long non-coding RNAs, there are some general features that are specific to lncRNAs only. LncRNAs are usually shorter and consist of longer exons, expressed in lower levels compared to protein coding genes and show less evolutionary conserved sequence pattern (9), (10). In contrast, some of the lncRNAs show unusual features such as, >100 kb length, high abundance in cells and sub-nuclear localization patterns. Altogether, lncRNAs are long transcripts which do not code for proteins and contain vast diversities in context of its structure, biogenesis and function (8).

1.1.2 LncRNA: Biogenesis and Functions

The biogenesis of lncRNAs includes transcription, post-transcriptional processing, localization and degradation (15) (Fig.1). Genome wide expression profiling studies demonstrate that lncRNAs are expressed more specifically in individual cell types, tissue types, developmental stages and in disease-specific manner (31) (3). Although most of the lncRNA sequences are not highly conserved, their promoter sequences have shown conservation patterns similar to that of mRNA promoters (11)(9)(7). The tissue and cell specific expression profiles of lncRNAs have made them promising candidates as markers of different developmental states like T cell differentiation (12) and embryonic development (13), and diseases like Cancers (14).

Long non-coding RNA genes exhibit similar chromatin modifications as protein coding genes such as H3K9ac, H3K27ac and H3K4me3. However, contrary to its protein coding genes, lncRNAs have shown a tendency to be regulated as a group. For instance, Dicer1 and MYC are involved in transcription regulation of hundreds of lncRNAs (15) (figure 1). Furthermore, lncRNAs can be transcribed as a result of divergent transcription from eukaryotic bidirectional mRNA promoters, which are commonly called upstream antisense (uaRNAs) (16). Previous studies have revealed that these mRNA-uaRNA pairs show a co-expression pattern which means that higher level of an mRNA indicates higher level of the uaRNA expression (16). Although RNAs can be transcribed in both directions, successful transcriptional elongation mostly occurs in the sense direction (17). In nearby sense direction, U1 snRNP splicing signals and polyadenylation signals (PAS) are enriched in the sequences as U1- PAS axis. U1 splicing signal sequences prevent early termination and enhance efficient elongation of mRNAs. However, nearby antisense direction transcripts are

mainly enriched with PAS, which favors polyadenylation and termination of uaRNAs (18) (figure 1)

During post transcriptional processing, most of the lncRNAs follow canonical events like 5'-capping, splicing, polyadenylation and chemical base modification (19). However, some exceptions follow non-canonical post-transcriptional processing. For instance, MALAT1 and NEAT1 contains tRNA-like structural elements at the 3' end forming a stable triple helix. RNase P cleaves these tRNA-like structures from NEAT1 and MALAT1 and generate mature RNAs (20).

Emerging studies show that lncRNAs commonly localize in specific subcellular regions of the cell. For instance, XIST (11), HOTAIR (21), NEAT1 (22), PVT1 (23) and MALAT1 (24) localize in the nucleus (25). Some other lncRNAs such as NORAD (26), lincRNA-p21 (27) and NKILA (28) are predominantly localized in the cytoplasm (25). Previous studies showed that lncRNAs are mostly present in the nucleus, especially in the chromatin fraction compared to the cytoplasmic fraction (9). However, recent studies on comparative analysis of lncRNAs and ribosome interactions suggest that lncRNAs are localized in every sub-cellular compartment of the cell and is particularly enriched in the cytoplasmic fraction (29). Altogether, it is obvious from these studies that lncRNAs are abundant in every sub-cellular area of the cell.

In general, stability of lncRNAs is similar to that of mRNAs and most of them follow canonical nonsense-mediated decay (NMD). lncRNAs commonly contain weak open reading frames (ORFs) and 3'-UTR like sequences which may activate NMD pathways. More specifically, cytoplasmic lncRNAs, such as GAS5, have similar characteristics like mRNA and are usually degraded through the canonical degradation pathway.

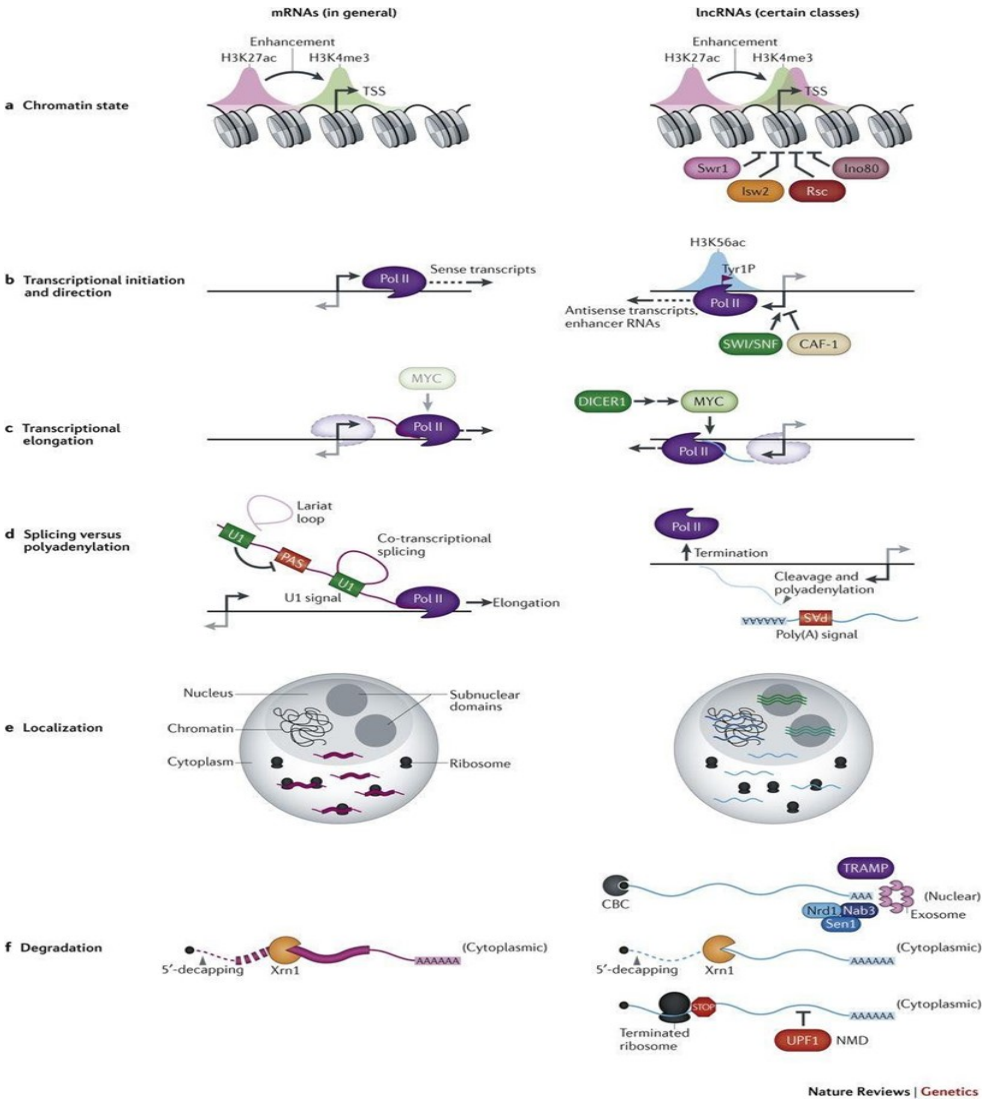

Figure 1: Biogenesis of long non-coding RNAs.

Some lncRNAs can be regulated differentially at transcription, maturation or degradation stages. (A) In chromatin stage, some lncRNAs have higher H3K27ac and strongly repressed by certain remodeling complexes. (B) Divergent promoter with enrichment of H3K27ac and phosphorylation of RNA pol II regulates some lncRNAs expression. (C) lncRNAs are more strongly regulated by MYC and DICER1. D. U1- PAS axis favors mRNA splicing in sense direction. (E) localization of lncRNAs are diverse. (F) lncRNAs mainly degraded by NMD pathway. Source: Quinn, Jeffrey J., and Howard Y. Chang. "Unique features of long non-coding RNA biogenesis and function." Nature Reviews Genetics 17, no. 1 (2016): 47.

1.1.3 microRNA: Biogenesis and Functions

MicroRNAs (miRNAs) are a class of small non-coding RNA with a length of about 23 base pairs. miRNAs are involved in the regulation of gene expression at the post transcriptional level by pairing with mRNAs of protein coding genes and inhibiting their translation (30). miRNAs can be found all over the genome. Although, majority of the miRNAs are generated from intronic regions of coding genes and are regularly transcribed along with their parental genes, some miRNAs can also be located as independent genes and their transcriptions are regulated by their own promoters. Furthermore, miRNAs can be transcribed as an independent self or as a polycistronic cluster which may generate multiple mature miRNAs (31). Although some of the miRNA genes are transcribed by RNA polymerase III, majority of them are transcribed by RNA polymerase II to generate the primary miRNAs (pri-miRNAs). These primary miRNAs are processed in the nucleus to produce the precursor miRNAs (pre-miRNAs) by a microprocessor complex consisting of Drosha and DGCR8. However, intronic miRNAs are processed by splicing events independent of the Drosha-based processing. These pre- miRNAs are then exported to the cytoplasm and cleaved by Dicer to generate two mature miRNA strands which are commonly referred to as the 5p' and 3p' strands (31)(32).

miRNAs may repress target mRNAs through mRNA degradation, translational repression, or acting as mRNA decoy. Complementary binding between the miRNA and mRNA induces an Ago2-based mRNA degradation through formation of RISC (RNA Induced Silencing Complex). When they are not complementary, miRNA based gene silencing is mediated by translational inhibition.

1.2 Prostate Cancer

1.2.1 Epidemiology of Prostate Cancer

Prostate cancer (PCa) is the most prevalent cancer and the second most common cause of cancer related deaths of American men (33). An estimated 164,690 new cases of PCa were diagnosed and 29,430 patients out of them died from this deadly cancer in 2018 in the United States (34) (Figure 3). According to the American Cancer Society, 1 out of 9 American men will be diagnosed with PCa in their lifetime. The 5 year survival rate for early stage (localized) prostate cancer is nearly 100%. However, late stage (metastatic) PCa has a 5 year survival rate of only 30% of the total cases diagnosed (35) (Fig. 2). According to this cancer statistics, metastasis remains the number one cause of PCa related deaths.

PCa is widely considered an elderly disease as it is rarely seen in men younger than 40 years with about 6 out of 10 cases in men aged 65 years or older. The average age of developing PCa is 66 years (35). Some of the risk factors include aging, race or ethnicity and family history. Additionally, unhealthy diets, smoking and obesity may further increase the risk of PCa incidence. According to the statistics of the American Cancer Society, African Americans and Caribbean population most commonly develop PCa compared to men from other ethnicity (35).

Prostate glands produce seminal fluid which nourish and transport sperms. Prostate cancer originates from the prostate gland and more than 95% of prostate cancer are adenocarcinomas. Prostatic intraepithelial neoplasia (PIN) is defined as the neoplastic growth of epithelial cells within benign prosthetic ducts or acini. Prostate adenocarcinoma is often found to be colocalized with prostatic intraepithelial neoplasia and high-grade PIN is most commonly accepted as a

precursor of prostate adenocarcinoma. Only a small percentage of prostate cancer patients develop other types of cancer in the prostate gland such as small cell carcinoma, neuroendocrine carcinoma and sarcoma.

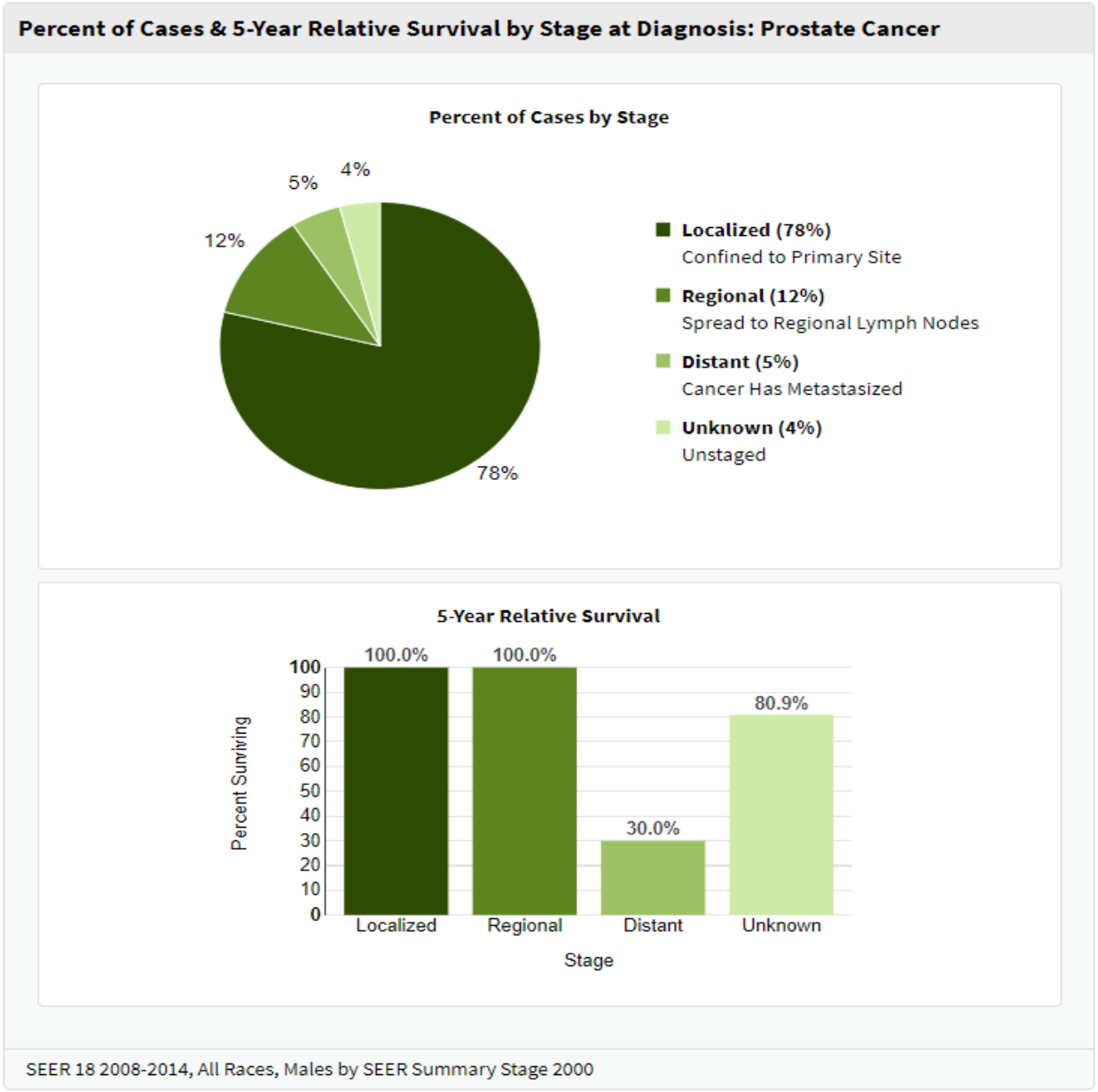

Figure 2: Statistics of 5 years survival rate of prostate cancer patients.

Source: SEER Cancer Statistics Review, 1975-2015, National Cancer Institute. Bethesda, MD.

	Common Types of Cancer	Estimated New Cases 2018	Estimated Deaths 2018
1.	Breast Cancer (Female)	266,120	40,920
2.	Lung and Bronchus Cancer	234,030	154,050
3.	**Prostate Cancer**	**164,690**	**29,430**
4.	Colorectal Cancer	140,250	50,630
5.	Melanoma of the Skin	91,270	9,320
6.	Bladder Cancer	81,190	17,240
7.	Non-Hodgkin Lymphoma	74,680	19,910
8.	Kidney and Renal Pelvis Cancer	65,340	14,970
9.	Uterine Cancer	63,230	11,350
10.	Leukemia	60,300	24,370

Figure 3: Statistics of cancer incidences and mortality from different cancer.
Source: SEER Cancer Statistics Review, 1975-2015, National Cancer Institute. Bethesda, MD.

When a patient is diagnosed with prostate cancer, it is important to determine how far the cancer has spread to other parts of the body and the stage of the cancer to plan the most suitable treatment option. The stage can be determined based on the results of diagnostic tests. The most prevalently used staging system is AJCC (American Joint Committee of Cancer) TNM system which is based on 5 key pieces of information including the extent of primary tumor (T), whether the cancer has spread to the nearby Lymph nodes (N), whether the cancer has metastasized to other organs (M), the grade group based on Gleason Scores and PSA levels during the diagnosis (36). The Gleason Score is commonly used to determine the progression of prostate cancer. In the early stage of prostate cancer, tumor tissues look well differentiated and limited as small glandular structure. As

the tumor progresses or spreads to other parts of the body, the tissue becomes less differentiated and basal cells are increasingly reduced as the tumor starts to infiltrate to neighboring areas. The Gleason Scores are lower for well differentiated tissue structure and gradually increases as the tissue structure become less differentiated (37) (Figure 4).

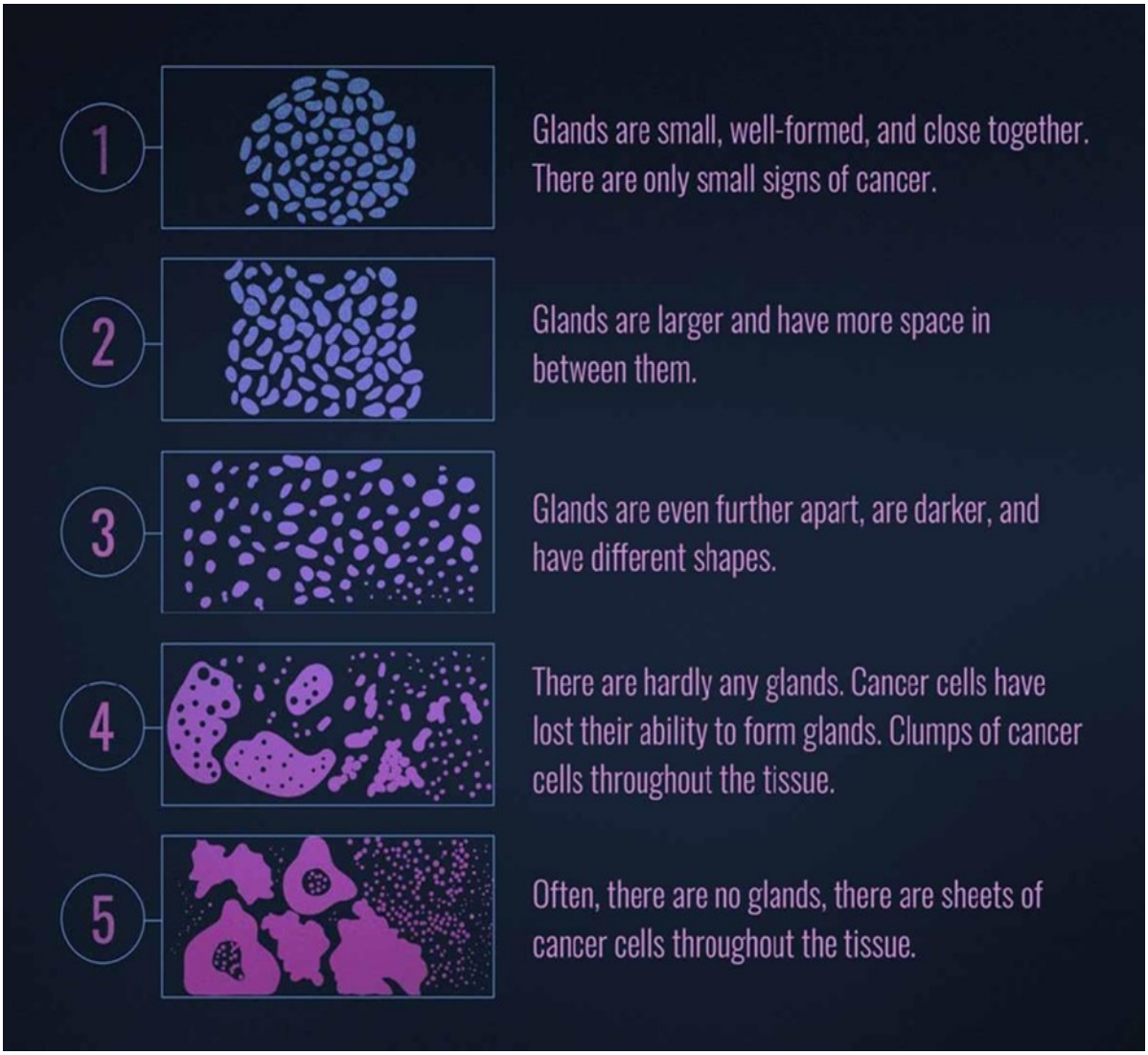

Figure 4: Gleason Scoring System classification.

Source: ProstateCancer.Net

1.2.2 Therapeutic Strategies

The course of prostate cancer progression is generally very slow, and patients might not need any treatment for their cancer. Doctors usually recommend the approaches commonly known as watchful waiting or active surveillance. Watchful waiting is mainly based on the less intensive follow-up and monitoring the changes of patient symptoms. On the contrary, active surveillance is a more intensive monitoring with different diagnostic tests like prostate specific antigen (PSA) level tests and prostate biopsies (38). Most widely practiced prostate cancer treatments are radical prostatectomy, radiation therapy, chemotherapy, cryotherapy, hormone therapy and immunotherapy.

1.2.3. Androgen Independence and Drug Resistance of Prostate Cancer

Prostate cancer development and progression are primarily dependent on androgen receptor signaling pathway. Androgens working through androgen receptor are required for maintenance of the normal prostate and cancerous prostate glands. As a consequence, androgen deprivation therapy is widely used as the standard of care for prostate cancer management, which may significantly inhibit prostate cancer growth and progression (39). Although initially prostate cancer patients respond to androgen deprivation therapies, eventually most of them develop resistance to these therapies and experience relapse with a more aggressive prostate cancer phenotype known as castration resistant prostate cancer (CRPC) (40).

Several pioneering studies elucidated the mechanisms of CRPC and revealed multiple mechanisms that may contribute to this stage. One of the prominent finding is that prostate cancer acquires the ability to circumvent androgen deprivation therapies by gaining hypersensitive activity to low level

of androgen (39). Castration resistant prostate cancer can achieve this feature in several ways such as androgen receptor (AR) amplification and increased AR sensitivity (39). Accumulation of the mutations in AR can change the binding specificity of ligands and can result in AR activation by other non-androgen steroids (39). Furthermore, recent studies demonstrated that AR can be activated through phosphorylation by MAPK and AKT pathways in the absence of androgen (41). Additionally, emerging evidences demonstrate aberrant expression of many cancer related genes in CRPC compared to androgen sensitive cancers which may contribute to the higher survival potential and aggressive behavior of CRPC cancer cells (42). It is obvious from these studies that aberrant expressions of not only protein coding RNAs but also non-coding RNAs can play a major role in the development of aggressive prostate cancer phenotypes. Therefore, non-coding RNAs, especially long non-coding RNAs and miRNAs gained tremendous attention as potential diagnostic and therapeutic targets.

1.3 LncRNA and Cancer

Genomic and transcriptomic projects demonstrated that aberrant expressions of non-coding genes are strongly correlated with changes in the expression of protein coding genes in cancer. Some of these lncRNAs play significant roles in the regulation of cancer hallmarks including evading apoptosis, metastasis and uncontrolled proliferation (43). These lncRNA genes can act as oncogenes or tumor suppressor genes directly or indirectly via interacting with other proteins in all levels of epigenomic regulations from chromatin remodeling to post-translational modifications (44) (45).

It is obvious from previous studies that some of the lncRNAs are overexpressed in cancerous tissues and play a role as oncogenes by promoting cancer phenotypes. For instance, H19, one of the well-studied oncogenic lncRNAs, is overexpressed in various cancers including breast, hepatocellular and colorectal cancers (46)(47). Another well studied lncRNA is HOX antisense intergenic RNA (HOTAIR), which is involved in the recruitment of polycomb repressive complex (PRC2) thereby promoting tumor invasion and metastasis in several cancers (48)(21). Additionally, MALAT1, a metastasis associated nuclear lncRNA, is overexpressed in lung cancer, and acts as a driver of metastasis and cell cycle progression in several cancer types including lung, breast and prostate cancer (49)(50).

Some of the lncRNAs, on the other hand have shown tumor suppressor properties by preventing cancer development and progression. For example, GAS5 (growth arrest-specific 5) is one of the most highly expressed lncRNAs in human tissues and is involved in embryogenesis (51). GAS5 is significantly down-regulated in several cancers such as breast, prostate, pancreatic and cervical cancer. Overexpression of GAS5 in xenografts of breast cancer cell lines in nude mice induced

apoptosis and cell cycle arrest (52). Some lncRNAs down regulate tumor suppressor genes and contribute to tumor progression. ANRIL is one such lncRNA that plays an oncogenic role by repressing neighboring tumor suppressor genes and promoting cell proliferation and invasion (53). Another lncRNA, lincRNA-p21, binds to MDM2 and can enhance p53 transcriptional activity in cancer cells and is also involved in cell cycle and cellular reprogramming (43)(45). Additionally, some lncRNAs can be regulated by tumor suppressor genes and may play functional roles in inhibition of cancer progression. For example, p53 regulates lncRNA PINT, which can act as an enhancer of p53-regulated transcriptional responses. PINT is down regulated in primary colon cancer and potentially act as a tumor suppressor by inhibiting proliferation of colon cancer cells (54).

1.3.1 LncRNA and Prostate Cancer

A number of long non-coding RNAs are noted to be dysregulated in prostate cancer that can act as oncogenes and tumor suppressor genes and may have significant contribution in the outcome of prostate cancer. These dysregulated lncRNA genes can act as regulators of all the hallmark. properties of prostate cancer. For instance, differentiation antagonizing non-protein coding RNA (DANCR) is highly expressed in prostate cancer tissues compared to respective adjacent uninvolved tissues and promotes prostate cancer metastasis by downregulating the metastatic inhibitor TIMP2/3 (55). PCa gene expression marker 1 PCGEM1, is found to be overexpressed in about 84% PCa patients (56) and its overexpression promotes proliferation and colony forming capacity of LNCaP prostate cancer cells (57). PCGEM1 regulates cell cycle related protein E2F and is involved in S phase progression. Furthermore, PCGEM1 regulates tumor metabolism via c-Myc activation. HOTAIR is another lncRNA that is upregulated in CPRC and activates AR in an

androgen independent manner. It has been found that HOTAIR acts as a driver of prostate cancer progression by promoting cell proliferation and invasion of CPRC (48). One of the well-studied lncRNA, SChLAP1, is overexpressed in prostate cancer tissues and in aggressive prostate cancer cell lines PC-3 and DU-145. SChLAP1 promotes aggressiveness of prostate cancer by antagonizing SWI/SNF complex (58). SChLAP1 also promotes migration and invasion by upregulating VEGF (vascular endothelial growth factor and MMPs (membrane metalloprotease) (59). Studies showed that another lncRNA MALAT1 is overexpressed in human prostate cancer and silencing of MALAT1 significantly delayed tumor growth and inhibited tumor metastasis. That study indicated that MALAT1 is involved several cellular processes including RNA splicing, nuclear organization and epigenetic modification (24).

Another lncRNA, MEG3 (maternally expressed gene 3), on the other hand, acts as a tumor suppressor in prostate cancer. MEG3 is significantly down regulated in prostate cancer tissues and overexpression of this lncRNA halted cell cycle progression by decreasing cell population in the S phase. MEG3 act as a tumor suppressor by activating p53, reducing expression of Bcl-2 and cyclin D1, enhancing Bax expression and activating Caspase-3 (60). Another tumor suppressor lncRNA, lincRNA-p2, is involved in prostate cancer and found to be downregulated in prostate cancer tissues. Overexpression of lincRNA-p2 can increase expression of p53 and induce cell death in prostate cancer cells (45). Additionally, it was elucidated that lincRNA-p21 promotes upregulation of a set of p53 regulated genes including Puma, Mdm2, Noxa and Bax and plays a role in inducing apoptosis of cancer cells (61).

1.3.2 Therapeutic Potential of LncRNAs

Emerging evidences shows that long non-coding RNAs play a vital role in cancer pathogenesis (62) and, have been considered as potential therapeutic targets for personalized treatments. As therapeutic strategies involving lncRNAs, so far, nucleic acid-based therapeutics is the most widely explored strategy to modify target RNAs at a post-transcriptional level. The advantage of this strategy is that nucleic acid-based drugs can target unique regions of the transcripts which is currently impossible with antibodies or other small molecule-based therapeutics (44). Two commonly used nucleic acid-based therapeutic approaches are RNA-mediated interference (RNAi) and anti-sense oligonucleotides (ASO) (44).

Several pharmaceutical companies such as Alnylam Pharmaceuticals, Ionis Pharmaceuticals and Merck Pharmaceuticals are actively involved in developing RNAi based therapeutics. However, these RNA molecules are susceptible to cellular nucleases (63) which makes it difficult to generate effective drugs. Although recent technological advancement allows for more stable RNAs, there are still many challenges that need to be addressed. Traditional siRNAs have been efficiently used to knock down many lncRNAs, such as MALAT1 (64) and HOTAIR (21), in different cell lines (Figure 5). However, siRNA mediated knockdown of these lncRNAs in vivo were not promising in most of the cases (44). Limited bioavailability in animals and lack of appropriate drug delivery methods are considered to be the major reasons for the failure of siRNA drugs in in vivo studies (65).

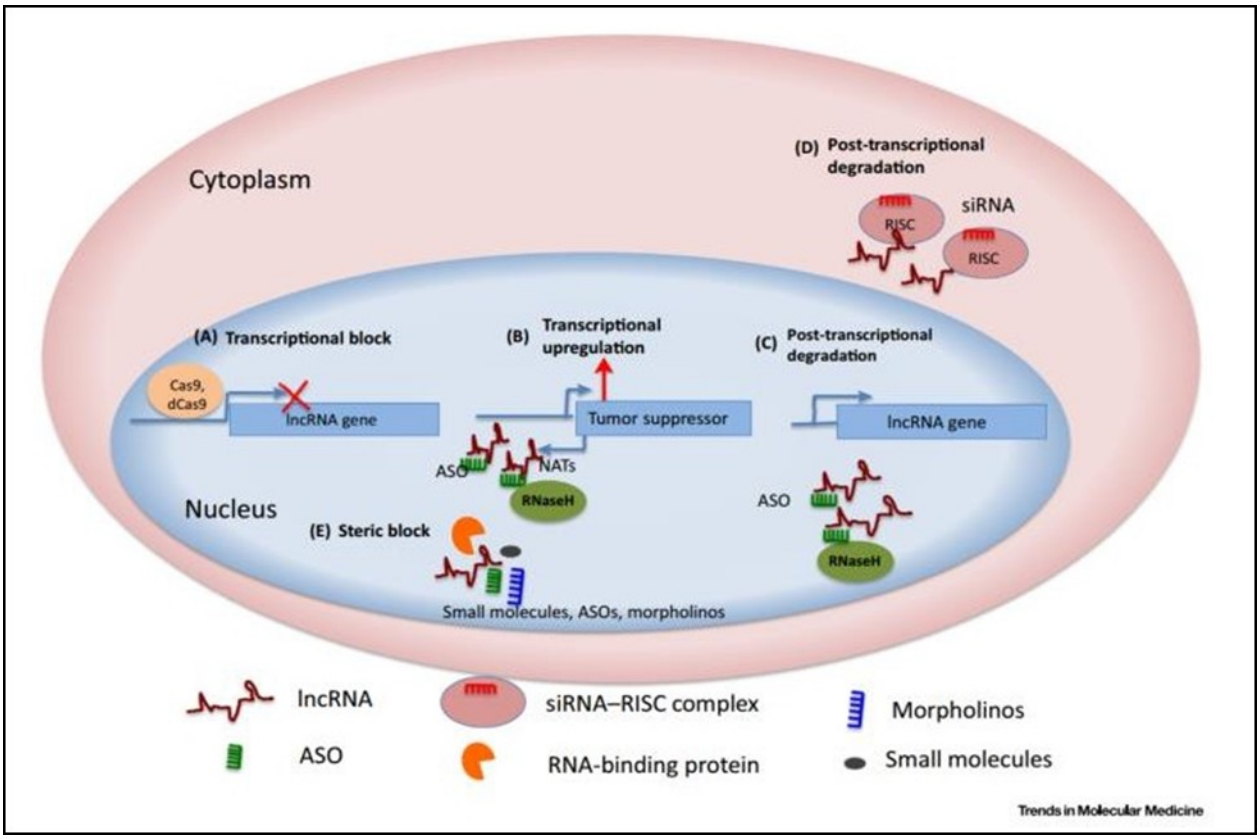

Figure 5: Different approaches to target lncRNAs in cytoplasm and nucleus.

(A) Transcriptional inhibition can be done by CRISPR/Cas9 based deletion. (B) Upregulation of tumor suppressor would be achieved by inhibition of natural antisense transcripts. (C) ASO can used to inhibit lncRNA function. (D) Post transcriptional silencing can be performed by siRNA. (E) Small molecules can be used to inhibit lncRNA-protein interactions. Source: Arun, Gayatri, Sarah D. Diermeier, and David L. Spector. "Therapeutic targeting of long non-coding RNAs in cancer." Trends in molecular medicine 24, no. 3 (2018): 257-277.

Recently, anti-sense oligonucleotides have been considered as the most promising nucleic acid based therapeutics. These ASOs directly bind to the target RNAs and can induce RNA degradation or may block their function by steric inhibition (66). ASO based therapeutics targeting mRNAs are currently under the process of evaluation in clinical trials for many deadly diseases including cancer (67). Recent studies showed that ASOs would be a promising therapeutic approach to target

lncRNAs (68) (Figure 5). One of the main advantages of ASO based therapeutics is that it can target RNAs in both nucleus and cytoplasm because of the abundance of RNase H in both regions. (69). As the majority of lncRNAs are enriched in the nucleus (70), these ASOs would be highly effective therapeutic agents to target lncRNAs. For instance, ASO mediated knockdown of MALAT1 reduced metastasis of breast cancer in mouse models (44) and reduced metastasis in lung cancer xenograft models. This study suggests a promising future for ASO mediated MALAT1 knock-down as an effective therapeutic strategy to prevent several cancer metastases.

Although there is a huge potential of nucleic acid based therapeutics, scientists still need to overcome some of the major obstacles. Delivery of these drugs into the cells is one of the burning issues that needs to be solved. Additionally, off-target effects of these nucleic acid based therapeutics need to be minimized in order to develop effective drugs with minimum side effects (44). Additionally, genome editing methods like CRISPR/Cas9 mediated CRISPR interference (CRISPRi) (71) have shown promising results in silencing blood cancer related lncRNAs like PVT1 and LUNAR1 and is being considered as a powerful therapeutic strategy targeting lncRNAs (72)(73) (Figure 5). In recent years, knock-down or inhibition of target molecules has become the most commonly practiced therapeutic strategies. Although there are not many studies involving overexpression of genes as a therapeutic strategy, it could prove to be crucial in diseases like cancer. Upregulation or activation of tumor suppressor genes could be harnessed to prevent cancer growth and progression (44). A subclass of lncRNAs, natural antisense transcripts (NATs) are transcribed from antisense direction and commonly overlaps with protein coding genes (74). Overexpression of these NATs regulate expression of overlapping protein coding gene as cis regulatory events (75)(76). Studies have shown that in several cancers, tumor suppressor genes are

suppressed by overexpression of the NATs (76). Many critical tumor suppressor genes overlap with these NATs. For instance, ANRIL overlaps with CDKN2B (77) and P21-AS overlaps with CDKN2A (78). Thus, in future, targeting these overexpressed NATs could be a promising therapeutic approach to restore the expression of the tumor suppressor genes.

Furthermore, steric inhibition of lncRNA binding with their target proteins by preventing the RNA-protein interaction could be another potential therapeutic strategy. Additionally, the high tissue specific expression of lncRNAs make their promoters to be encouraging DNA elements for therapeutic purposes. H-19 gene promoter-based diphtheria toxin subunit expression is being used to elicit anti-tumor response (79) and is currently under clinical trial phase I/IIa (80). Long non-coding RNAs have unique and stable secondary and tertiary structure (81), which could be used as potential therapeutic targets. For example, lncRNA MALAT1 has a triple-helical structure at the 3' end of the transcript (82) and this unique structure could be exploited to a therapeutic advantage. Using appropriate small molecular inhibitors, these unique structural features of lncRNAs could be destabilized or allosterically interfered to prevent their binding to target proteins. All these pioneering studies indicate that lncRNAs would be promising candidates as therapeutic targets in cancer in the context of nucleic acid based therapeutic platform.

1.4 microRNA and Prostate Cancer

miRNAs are commonly dysregulated during the development and progression of several cancers including prostate cancer (83). Emerging evidences suggest ectopically expressed miRNA often act as oncogenes, whereas downregulated miRNAs act as tumor suppressors in cancers. However, there are some miRNAs which have dual roles as both oncogenic and tumor suppressive in

different context. These miRNAs may play their tumor suppressor or oncogenic role based on the specific cell types (84). miRNAs are involved in promoting cancer phenotypes including abnormal cell proliferation, apoptosis inhibition and increased invasive or cancer stem cell like properties (85). For instance, miR-34a is involved in promoting apoptosis, and miR-21 and miR-200 are involved in cancer cell proliferation and metastasis (86).

Aberrantly expressed miRNAs may play a significant role in the incidence and progression of prostate cancer (87). For instance, miR-200 and let-7 are downregulated in aggressive prostate cancer and may induce epithelial mesenchymal transition (88)(89). Ectopic expression of miR-34a may induce cell cycle arrest and reduce drug resistance in prostate cancer cells. Furthermore, androgen receptor regulates more than hundreds of miRNAs including let-7g, -15a, , 17-5p, -19b, -20a, -21, -106a, -148a in prostate cancer (90). Additionally, some of the miRNAs may directly target and regulate AR expression such as 34c, -299-3p, and -135b, -541(79)(91). These AR regulated and AR targeting miRNAs may further contribute to prostate cancer progression. For example, miR-17 regulates a coactivator of AR, p300/CBP and thereby regulates AR activity (92).

Previous studies in our lab demonstrated that a polycistronic miRNA cluster, miR-17-92a is downregulated in prostate tumor tissues and collectively plays a tumor suppressor role in aggressive prostate cancer cells. Restoration of miR-17-92a reduced cell proliferation and expression of cell cycle regulatory protein Cyclin D1, SSH1, LIMK1 and FGD4. Restoration of miR-17-92a also reduced cell migration and altered expression of epithelial mesenchymal transition markers and surface localization of epithelial marker E-cadherin. Additionally, miR-17-92a expression in both androgen sensitive and resistant prostate cancer cell lines, showed an improved sensitivity of these cells to several prostate cancer drugs such as anti-androgen drug

Casodex, Akt inhibitor MK-2206, Aurora kinase inhibitor VX-680, chemotherapeutic agent Docetaxel (93).

CHAPTER TWO: HYPOTHESIS AND SPECIFIC AIMS

Previous studies in our lab showed that miRNA polycistronic cluster miR-17-92a, located in the third intron of the C13orf25 transcript, is frequently downregulated in prostate cancer tissues compared to adjacent normal prostate tissues. miR-17-92a cluster transcript generates six mature miRNA miR-17, -18a, -18b, -19b, -20a and -92a. Restoration of expression of all members of miR-17-92a cluster simultaneously in prostate cancer cells showed decreased cell proliferation and cell migration, delayed tumorigenicity, and increased sensitivity of AR antagonist Casodex, Akt inhibitor MK-2206, Aurora kinase inhibitor VX-680 and chemotherapeutic agent Docetaxel. Transcriptome profiling of PC-3 prostate cancer cell line expressing miR-17-92a cluster miRNAs revealed altered expression of several coding and non-coding RNAs, especially lncRNAs including NONHSAT036820 (LINC00888), NONHSAT201120 and NONHSAT221895 compared to PC-3 cell line expressing scramble RNAs. We focused our study on most downregulated intergenic lncRNA LINC00888 and annotated it as PAINT (Prostate Cancer Associated Intergenic Non-coding Transcripts). Furthermore, in silico based expression analysis showed that PAINT is differentially expressed in many cancers, including metastatic colon cancer, lung cancer, melanoma and breast cancer. Our analysis further revealed PAINT to be ectopically expressed in all prostate cancer cell lines derived from distant metastasis. GEO database analysis showed that androgen deprivation therapy increased expression of PAINT in androgen sensitive LNCaP prostate cancer cell line. Because PAINT showed aberrant expression in different cancers including aggressive prostate cancer and prostate cancer cell lines, we selected PAINT from our list of altered lncRNAs for further study.

We hypothesize that reduced expression of PAINT as a result of restoration of expression miR-17-92a cluster miRNAs is associated with the tumor suppressor function of miR-17-92a cluster in prostate cancer and upregulation of PAINT is involved in prostate cancer progression. In this study, we aim to define the association of PAINT with prostate cancer and functionally characterize PAINT as an oncogene by pursuing the following aims.

2.1 Aim 1. Study the expression level of PAINT in prostate cancer cells lines and tumor tissues.

In this aim, we plan to study the expression of PAINT in prostate cancer cell lines using qRT-PCR. Here, we will use a variety of prostate cancer cell lines such as PC-3 and MDA-PCa-2b (derived from bone metastatic site); LNCaP (derived from lymph node metastatic site); C4-2B (castration resistant prostate cancer cell line derived from LNCaP cells); 22Rv1(prostate cancer cell line with mutated androgen receptor) and RWPE-1 (normal prostate cancer cell line) (94). We will confirm the inverse expressional relationship of PAINT with miR-17-92a miRNA cluster by overexpressing miR-17-92a mature miRNAs in PC-3 cell line using qRT-PCR. We will also study the expression pattern of PAINT in clinical specimens. RNA in-situ hybridization (RNA-ISH) will be performed to analyze PAINT expression using tissue microarray (TMA) slides containing prostate cancer tissues of different stages and normal prostate tissues.

2.2 Aim 2. Examine the function of PAINT in prostate cancer cells

In this aim, we will study the function of PAINT using overexpression and silencing approaches in prostate cancer cells. We will select our *in vitro* models based on the endogenous expression of PAINT with cell lines having high expression of PAINT being selected for gene silencing studies and cell lines with low PAINT expression being selected for overexpression studies. We will

explore the role of PAINT in modulating prostate cancer cell phenotypes through studies involving cell proliferation, cell cycle progression, cell survival, cell migration and expression of protein associated with these phenotypes.

CHAPTER THREE: MATERIALS AND METHODS

3.1 Analysis of RNA seq Data and Criteria for Selection of LncRNAs

Whole genome transcription except small RNAs such as ribosomal RNAs (rRNAs) and transfer RNAs (tRNAs), profiling was performed in a PC-3 subline expressing either all six miR-17-92a cluster or scramble RNA. Differential expression of lncRNAs were analyzed based on a minimum of $\log_2$ 2 fold change of expression between these two PC-3 sublines. For further study, the top 3 candidates of lncRNAs were determined based on their intergenic positions in the genome, their expression cut-off value of at least 20 FPKM (Fragments per kilobase per million) in at least one of the sublines and a change of expression greater than Log_2 2 fold.

3.2 Structural Analysis and In-silico Analysis of PAINT Expression in Tissues.

NONCODE and UCSC Genome Browser were used to identify the locations and genomic structures of the selected long non-coding RNAs. Preliminary data of the differentially expressed lncRNAs such as genomic lengths, transcript lengths, intergenic positions, neighboring genes and expression profiles in different tissues were collected in order to better define the selected lncRNAs. Furthermore, in silico expression analysis was performed to determine their expression in different cancers and cancer cell lines. Several databases such as cBioPortal, EMBL Expression Atlas, NCBI GEO profiles and previously published studies were also used in the expression analysis.

3.3 Cloning and Purification of PAINT

The 1.7kb spliced transcript of PAINT was cloned by GenScript cloning services. PAINT spliced transcript was cloned in the multiple cloning site (MCS) of the pcDNA3.1+ mammalian expression

vector (GenScript) and was transformed into XL-10 ultra-competent *E. coli* cells for the isolation of single colonies. For the transformation process, competent cells were thawed on ice and subsequently, 100 µL of competent cells were transferred into the pre-chilled 12 x 75 mm Falcon tubes. Next, 50 ng of the closed plasmid was added to the cells and gently mixed. This mixture was then incubated on ice for 30 minutes followed by heat-shock at 42^0C for 45 seconds. Following the heat-shock, the tube was placed back on ice for 2 minutes. Next, 500 µL of pre-warmed LB broth was added to the cells and incubated at 37^0C with shaking at 250 rpm, for one and half hours. Finally, 50 µL cells were plated on LB agar plate containing 100 µg/mL ampicillin and incubated overnight (16 – 18h) in a 37^0C incubator. Next day, single colonies were picked to make streak plates and to start a bacterial culture by inoculating in 3 mL of LB broth containing 100ug/ml Ampicillin. The bacterial cultures were incubated in a shaking incubator at 37^0C with shaking at 250 rpm overnight (16 -18h) and used for plasmid DNA extraction.

Boiling minipreps were performed initially to screen the selected colonies for the presence of the plasmid DNA. 1.5 mL of the overnight grown cultures was transferred to microcentrifuge tubes and centrifuged at 12,000 xg for 30 seconds at room temperature. The supernatants were discarded, and the same step was repeated one more time to pellet all the cells from the 3 mL inoculated cultures. Pelleted cells were then resuspended in 350 µL of plasmid lysis buffer (8% Sucrose, 0.5% Triton X-100, 50 mM EDTA with pH 8.0 and 10 mM Tris-Cl with pH 8.0) containing 25 µL of freshly prepared lysozyme solution (10 mg/mL in plasmid lysis buffer) and 0.5 µL of RNase solution (10 mg/mL). The tubes were then incubated on ice for 5 minutes followed by boiling for 1 minute to denature the genomic DNA. The tubes were immediately centrifuged for 15 minutes at 12000 xg at room temperature. The genomic DNA pellet was removed and the supernatant

containing the plasmid DNA was transferred to a fresh tube. To the supernatant, 33 µL of 3M Sodium Acetate (pH 5.5) and 430 µL of Isopropanol were added, mixed by vortexing and incubated at room temperature for 5 minutes. The tubes were centrifuged for 12000 xg for 5 minutes at room temperature and the supernatants were discarded. Restriction digestions were performed at 37^0C (20 µL reaction volume containing 2 µL of 10x CutSmart buffer, 0.5 µL BamHI-HF, 0.5 µL KpnI-HF, 500 to 1000 ng DNA and nuclease-free water) followed by agarose gel electrophoresis to identify the colonies containing the plasmid DNA. A glycerol stock was made for each construct using 1 mL of the overnight culture and 500 µL of 50% glycerol solution which was stored at -80^0C for future use.

To extract transfection-quality plasmid DNA from the positive colony, a culture was started by inoculating 3 mL of LB broth containing 100 µg/mL ampicillin from the previously-made glycerol stock for that specific colony and incubated overnight (16 - 18h) with shaking at 250 rpm, 37^0C. The following day, DNA was extracted using the PureYield Plasmid Spin Miniprep kit from Promega as per the manufacturer protocol. All centrifugation steps were performed at 13000 xg and at room temperature unless otherwise mentioned. Briefly, the overnight cultures were centrifuged, and the pellets were resuspended in 600 µL of deionized water. Next, 100 µL of the Cell Lysis Buffer reagent was added to the suspension and inverted 5 to 6 times to ensure complete mixing. This was followed by the addition of 350 µ of cold (4-8^0 C) Neutralization Buffer Solution and mixed by inversion until the complete neutralization of lysis buffer was achieved. The tubes were then centrifuged for 3 minutes and 900 µL of the supernatant was transferred to pre-wetted PureYield mini column. This was then centrifuged for 15 seconds and the flow-through was discarded. The mini column was washed with 200 µL Endotoxin Removal Wash Solution followed

by centrifugation for 15 seconds and the flow-through was discarded. This was followed by another wash step with 400 µL Column Wash Solution and centrifuged for 30 seconds. Finally, the plasmid DNA was eluted into a fresh microcentrifuge tube by adding 30 µL Elution Buffer to the center of the mini column, incubated at room temperature for a minute followed by centrifuging for a minute. The eluted plasmid DNA was checked by restriction digestion as previously described and was stored at 4^0C until further use.

3.4 Cell Culture

PC-3 prostate cancer cell line (ATCC) was cultured in F-12 Kaighn's Modification HAM medium (Sigma Aldrich) containing 10% heat-inactivated Fetal Bovine Serum (FBS) (Atlanta Biologicals) and 1% antibiotic/antimycotic (Life technologies) in a 37^0C CO_2 incubator with 5% CO_2. Cells were routinely sub-cultured roughly at 70-80% confluency 2 to 3 times per week. For sub-culturing, PC-3 cells were washed with PBS and were incubated with 0.05% trypsin EDTA solution (Life Technologies) for 3 minutes. Trypsin EDTA solution was then removed and the plates were incubated for 10 minutes at 37^0C incubator with 5% CO_2. After this incubation steps, the dissociated cells were resuspended with complete media and sub-cultured at a ratio of 1:3 or 1:4 with complete media.

C4-2B prostate cancer cell line (ATCC) was maintained in RPMI-1640 media (Sigma Aldrich) containing 10% heat-inactivated Fetal Bovine Serum (Atlanta biologicals) and 1% antibiotic/antimycotic (life technologies) at 37^0C in a CO_2 incubator with 5% CO_2. Cells were sub-cultured in 10 cm dishes at 75-85% confluency 2 to 3 times per week. C4-2B cells were washed with PBS and incubated with 0.05% trypsin EDTA solution (Life Technologies) for 3 minutes at

37^0C. After incubation, trypsin EDTA solution was removed and incubated again about 8 to 10 minutes at 37^0C. Trypsinized cells were resuspended and sub-cultured at 1:3 or 1:4 ratio in 10 cm tissue culture plates with complete media.

22Rv1 prostate cancer cell line (ATCC) was maintained in RPMI-1640 medium (Sigma Aldrich) containing 10% heat-inactivated Fetal Bovine Serum and 1% antibiotic/antimycotic (Life Technologies). 22Rv1 cells were passaged at 75- 85% confluency 2 times per week. Cells were washed with PBS and incubated with 0.05% trypsin EDTA solution in 37^0C incubator for 3 minutes. Next, trypsin EDTA solution was aspirated and culture plate was again incubated in 37^0C incubator for 5 to 10 minutes. Finally, cells were resuspended and sub-cultured at 1:3 ratio in complete media.

Androgen dependent LNCaP subline LNCaP-104S prostate cancer cell line (a gift from Dr. Shutsung Liao from University of Chicago) was sub-cultured in DMEM media (Sigma Aldrich) containing 10% heat-inactivated Fetal Bovine Serum and 1% antibiotic/antimycotic and 1 ng/mL Dihydrotestosterone (DHT) (Life technologies). Cells were sub-cultured approximately at 80% confluency 2 times per week. Briefly, cells were washed with PBS and incubated with 0.05% trypsin-EDTA solution (Life Technologies) for 30 seconds at room temperature. Next, trypsin-EDTA solution was removed and plate was incubated in 37^0C incubator for 3 to 5 minutes. Cells were resuspended with complete media and sub-cultured at 1:3 ratio with complete media.

MDA-PCa-2b cell line (ATCC) was maintained in 10% F-12K medium (Sigma Aldrich) containing 10% non-heat inactivated Fetal Bovine Serum, 1% antibiotic/antimycotic (Life Technologies), 25ng/mL cholera toxin, 10ng/mL mouse Epithelial Growth Factor, 0.005 mM phosphoethanolamine, 100 pg/mL hydrocortisone, 45nM sodium selenite, 0.005 mg/mL human.

recombinant insulins. Cells were sub-cultured roughly at 80% confluency 2 times per week. Cells were washed with PBS and incubated for 3 minutes with 0.05% trypsin-EDTA solution in 37^0C incubator. After that, trypsin EDTA solution was removed and plate was again incubated for 5 to 10 minutes in 37^0C incubator. Cells were resuspended with complete media and sub-cultured at 1:3 ratios with complete media.

RWPE-1 cell line was sub-cultured and maintained in Keratinocyte Serum Free Medium (K-SFM) (Gibco) supplemented with 0.05 mg/mL BPE and 5ng/mL EGF (provided with K-SFM kit). Cells were sub-cultured every two days at a 1:3 ratio. After removing media, cells were washed with PBS and incubated with 0.05% trypsin EDTA for 2 minutes in 37^0C incubator. Trypsin EDTA solution was removed and incubated for an additional 5 to 10 minutes in 37^0C incubator. Finally, cells were resuspended and sub-cultured with complete media.

3.5 Transfection

Prostate cancer cell line PC-3 were transfected with PAINT siRNA smart pool and non- targeting siRNA pool (Dharmacon) using RNAiMAX (Invitrogen) to perform knock-down study. PC-3 cells were seeded 24 hours before transfection to achieve a 70% confluency at the time of transfection. Media was changed 1 hour before transfection and incubated again in 37^0C incubator. In order to perform siRNA transfection, respective amounts of RNAiMAX reagent and siRNAs were diluted in Opti-MEM media (Thermo Fisher Scientific) and incubated for 2 minutes. Diluted PAINT siRNA smart pool and non-targeting siRNA pool was mixed with diluted RNAiMAX individually (Table 1) and incubated for 10 minutes. After 10 minutes of incubation, the transection mixture

was added dropwise into the wells. Media was changed 8 hours after transfection and incubated for a period of 48 – 72 hours after transfection in 37^0C incubator for the required experiments.

For other transfection experiments, C4-2B or PC-3 cells were seeded 24 hours before transfection to reach about 70% confluency at the time of transfection. Media was changed 1 hour before transfection and incubated again in 37^0C incubator. Lipofectamine 3000 (Invitrogen) was used to transfect cells (Table 2). Plasmid DNA, P-3000, and Lipofectamine 3000 reagents were diluted with Opti-MEM (Life technologies), incubated for 15 minutes at room temperature and added dropwise into the respective wells. Media was changed after 8 hours of transfection and incubated for 48 – 72 hours after transfection for the respective experiments. For PAINT overexpression studies, pcDNA3.1+PAINT was transfected into C4-2B cells to overexpress PAINT and pcDNA3.1+control was transfected into C4-2B cells as a negative control. For miR-17-92a overexpression studies, pLVX-TetOne-Puro-miR-17HG containing precursor DNAs for all six miRNAs in tandem was transfected into PC-3 cells to overexpress miR-17-92a cluster and pLVX-TetOne- Puro empty vector DNA was transfected into PC-3 cells as a negative control. The following table listed individual transfection mixtures for each of the transfected cell lines for respective 6, 24 and 96 well plates.

Table 1: Transfection protocol for RNAiMAX reagents.

Samples	Mixture A	Mixture B
6 well plates (for 1 well)	150 µL Opti-MEM 9 µL of RNAiMAX	150 µL Opti-MEM 10 µL of siRNA (10µM)
24 well plates (for 1 well)	25 µL Opti-MEM 1.8 µL of RNAiMAX	25 µL Opti-MEM 2 µL of siRNA (10µM)
96 well plates (for 5 well)	25 µL Opti-MEM 1.8 µL of RNAiMAX	25 µL Opti-MEM 2 µL of siRNA (10µM)

Table 2: Transfection protocol for Lipofectamine 3000 reagents.

Well plates	Mixture A	Mixture B
6 well plates (for 1 well)	125 µL Opti-MEM 3.5 µg DNA 2.5 µL p3000	125 µL Opti-MEM 3.75 µL Lipofectamine 3000
24 well plates (for 1 well)	25 µL Opti-MEM 0.75 µg DNA 0.5 µL p3000	25 µL Opti-MEM 0.75 µL Lipofectamine 3000
96 well plates (for 5 well)	25 µL Opti-MEM 0.75 µg DNA 0.5 µL p3000	25 µL Opti-MEM 0.75 µL Lipofectamine 3000

3.6 Isolation of Stable Cell Lines

C4-2B cells were transfected with pcDNA3.1+PAINT or pcDNA3.1+empty vector using previously described transfection protocol for Lipofectamine3000 reagents. 48 hours after transfection, cells were treated with 1 mg/mL of G-418 (KSE Scientific) (from 50mg/ml stock solution in water) on alternate days for a period of 3 weeks to select stably transfected C4-2B colonies. In order to select individual clones, cells were washed with PBS and micro disks (Fisher Scientific) prewetted with 0.05% trypsin EDTA solution were placed on the individual colonies. Plates were incubated in 37^0C incubator for 10 minutes and disks were transferred to separate wells of 24 well plates with 500 µL complete media containing 1 mg/mL G-418 and grown until individual colonies are formed. Cloning discs were discarded, and cells were maintained for continued growth. After cells reached 80% confluency, they were subsequently transferred to 6 well plates and then to 10 cm culture plates and grown to confluency with 1mg/mL G-418 containing complete media. Expression of PAINT was analyzed with qRT-PCR after the clones received confluency in the 10cm plates. pcDNA3.1+PAINT transfected clones that showed a >2-fold overexpression of PAINT were selected and expanded separately or as a group based on similar expression. pcDNA3.1+ empty vector transfected clones with similar expression of parental C4-2B cells were selected, mixed together and expanded as control population. After expansion, C4-2B sublines were used for experiments or frozen in liquid nitrogen for future studies.

3.7 RNA Extraction and cDNA Synthesis

RNA extraction was performed using the Direct-zol quick miniprep plus (Zymo Research) RNA extraction kit. To extract RNA from prostate cancer cell lines, cells were harvested and resuspended in complete media and centrifuged at 840 xg at 4^0C for 5 minutes. Media was discarded and cell pellets were washed again with PBS and centrifuged again at 840 xg for 5 minutes. Next, cells were lysed with Qiazol reagent (Qiagen) and total RNAs were extracted by following the manufacturer protocol. RNA concentration was measured using Nanodrop-1000 (Thermo Fisher Scientific) and either used immediately or stored at -80^0C until further use. To ensure extraction of high quality RNA, RNA with 260/280 ratio of 2.00 were used for all experiments.

cDNA synthesis was performed using RT^2 First Strand Kit (Qiagen) or High Capacity cDNA Synthesis kit (Applied Biosystems) or QuantiMir kit following recommended protocols. As recommended in the High-Capacity cDNA Reverse Transcription Kit (Applied Biosystems), 500 ng or 1 μg of purified total RNA was usually used as the starting material for cDNA synthesis. For cDNA synthesis with the High-Capacity cDNA Reverse Transcription Kit, we used 0.8 μL of 25x dNTP mix (100mM), 2 μL 10x RT buffer, 2 μL 10x random primer, 1μL reverse transcriptase, 4.2 μL nuclease free water and 10 μL RNA samples for a 20 μL reaction as per manufacturer protocol. The cDNA synthesis cycling conditions were as follows: step 1 - 25^0C for 10 minutes, step 2 - 37^0C for 120 minutes, and step 3 - 85^0C for 5 minutes. Synthesized cDNAs were diluted 1:5 and either used immediately or stored at -20^0C for future use. For the cDNA synthesis using RT^2 First Strand Kit recommended protocol, genomic DNA elimination mix was prepared in sterile PCR tube as 10 μL reaction (2 μL Buffer GE, 1 μg RNA in RNase free water) and incubated for 5

minutes at 42^0C followed by placing on ice for at least 1 minute. Next, reverse transcription mix was prepared in a 10 µL reaction (4 µL 5x Buffer BC3, 1 µL control P2, 2 µL RE3 Reverse Transcriptase mix and 3 µL RNase- free water) volume, which was then added to each tube containing genomic DNA elimination mix. After mixing by gently pipetting, the reaction was incubated at 42^0C for 15 minutes followed by an incubation at 95^0C for 5 minutes to stop the reaction. cDNAs were diluted 1:5 and either immediately used or stored at -80^0C for future use.

3.8 Quantitative Real Time PCR

Expression of miR -17-92a and PAINT was determined by quantitative real-time PCR in prostate cancer cell lines using QuantiMir Kit (SBI) and RT^2 lncRNA PCR array primer (Qiagen). For PAINT expression analysis, a 10 µL reaction volume containing 5 µL of 2x SYBR-green master mix, 1 µL of 10x RT^2 primer (Qiagen) and 2 µL of diluted cDNA was used for quantitative real time-PCR. Quantstudio 7 (Applied Biosystem) instrument was used to perform qRT-PCR for 40 cycles with the following cycling conditions: 95^0C for 10 minutes (1 cycle), 94^0C for 15 seconds, 55^0C for 30 seconds, 72^0C for 30 seconds (40 cycles). Expression of RPL13A and EIF3D genes were used as the internal controls. We have used RT^2 primers for all lncRNA and mRNA genes in this expression analysis.

For miR-17-92a expression analysis, a 10 µL reaction containing 5 µL of 2x SYBR Green qPCR Mastermix buffer, 1 µL Forward Primer (10 µM) (Table 3), 0.5 µL Universal Reverse Primer (10 µM) and 2 µL diluted cDNA was used in qRT-PCR. Quantstudio 7 (Applied Biosystem) instrument was used to perform qRT-PCR with the following cycling conditions: 95^0C for 10 minutes (1 cycle), 94^0C for 15 seconds, 60^0C for 1 minute (40 cycles). Expression of U6 snRNA,

RNU43 snoRNA, RNU1A snRNA were used as internal control. Data were analyzed with 2-ΔΔCT Livak-method to determine PAINT or miR-17-92a expression changes in control and experimental conditions whereas ΔCT values were used for determining endogenous level of expression.

Table 3: Primers used for miR-17-92a expression profiling using qRT-PCR

miRNA	Primer sequences
hsa-miR-17	CAAAGUGCUUACAGUGCAGGUAG
hsa-miR-18a	UAAGGUGCAUCUAGUGCAGAUAG
hsa-miR-19a	UGUGCAAAUCUAUGCAAAACUGA
hsa-miR-19b	UGUGCAAAUCCAUGCAAAACUGA
hsa-miR-20a	UAAAGUGCUUAUAGUGCAGGUAG
hsa-miR-92a	UAUUGCACUUGUCCCGGCCUGU

3.9 Whole Cell Protein Extraction and Immuno-Blotting

Prostate cancer cell lines were harvested for whole cell protein extraction by scrapping the cells on ice. Cells were washed 2x with ice cold PBS followed by centrifugation at 840 xg at 4^0C. Pellets were resuspended in RIPA buffer (25 mM Tris-HCl pH 7.6, 150 mM NaCl, 5 mM EDTA, 1% Triton X-100, 1% sodium deoxycholate, 0.1% SDS) containing 1x protease and phosphatase inhibitor cocktail (Fisher Scientific). Cell lysates were frozen in a dry ice-ethanol bath for 3 times and immediately thawed at 37^0C water bath with 15 second vortexing in between each cycle. Next, lysates were centrifuged at 13000 xg for 15 minutes at 4^0C and the supernatants were transferred to previously chilled microcentrifuge tubes. Protein concentration was measured by Bradford assay (Bio-Rad) and immediately used for polyacrylamide gel electrophoresis or stored at -80^0C for future use.

For protein separation, Bis-Tris SDS-PAGE (10% gels) or Bio-Rad mini gradient gels (4-20%) were used. 50 μg of protein samples was diluted with 6X Laemmli sample buffer and denatured by boiling at 100^0C for 10 minutes. The samples were then briefly centrifuged and loaded into the respective lanes in the gel. The gel was then run with a constant voltage of 100V (Bio-Rad gels) or a constant current of 0.06A (Bis-Tris Gels). Precision-Plus all blue protein standard (Bio-Rad) was also run for determining the size of the protein bands. Following the gel run, proteins were transferred to activated PVDF membrane using the Transblot Semi-Dry Transfer system (Bio-Rad). Separated proteins were transferred using 1x Transblot transfer buffer (100 μL of 5x Transblot transfer buffer + 100 μL of Absolute Ethanol + 300 μL deionized water) for 5 or 7 minutes at a constant current of 1.3A. Membranes were stained with India ink for 30 minutes and blocked for non-specific binding of proteins with 5% non-fat milk for 2 hours at room temperature. Membranes were then incubated with the respective primary antibodies with optimal dilutions in 5% milk or 1% casein overnight at 4^0C or for 1-2 hours at room temperature (Table 4). Unbound antibodies were washed off by washing the membrane in TBS-T for 15 minutes per wash for 3 wash cycles at room temperature. Membranes were than incubated with HRP conjugated secondary antibodies in 5% non-fat milk in TBS-T for 1 hour at room temperature. Unbound antibodies were washed with 1X TBS-T for 15 minutes per wash for 3 times. Chemiluminescent substrate was added to membranes and used to visualize positive signals using a ChemiDoc MP Imaging System. Protein band intensity was quantified by densitometric analysis using the ImageJ image analysis software and the intensity values were normalized to the paired value of GAPDH or alpha-tubulin loading control. The calculated normalized values were used to compare the fold change in expression of different target proteins.

Table 4: Dilutions of antibodies and incubation times.

Target protein	**Supplier company**	**Product no.**	**Host**	**Dilution factor**	**Incubation conditions**
SLUG	Cell signaling	9585S	Rabbit	1:100	4^0C; overnight
VIMENTIN	Cell signaling	5741S	Rabbit	1:100	4^0C; overnight
E-CADHERIN	Cell signaling	3195P	Rabbit	1:700	4^0C; overnight
N-CADHERIN	Cell signaling	13116S	Rabbit	1:250	4^0C; overnight
CLEAVED CASPASE-3	Cell signaling	9664S	Rabbit	1:100	4^0C; overnight
PARP	Cell signaling	9542S	Rabbit	1:100	4^0C; overnight
CLEAVED-PARP	Cell signaling	9542S	Rabbit	1:100	4^0C; overnight
ALPHA-TUBULIN	Cell signaling	2125S	Rabbit	1:1000	4^0C; overnight
GAPDH	Cell signaling	2118S	Rabbit	1:1000	4^0C; overnight
Rabbit IgG	Cell signaling	7074S	Goat	1:2000	4^0C; overnight

3.10 Cell Proliferation/Cytotoxicity Assay

MTS (Promega) colorimetric assays were performed to determine cell proliferation or cytotoxicity of prostate cancer cell lines following PAINT overexpression or knockdown. MTS is a tetrazolium compound which gets converted to formazan by NADPH or NADH dehydrogenase enzymes in metabolically active cell populations. This causes a color change from yellow to purple which can be quantified at 490nm wavelength. The intensity of the purple color is directly proportional to the amount of metabolically active cells. 96 well plates were seeded with the respective cell lines 24 hours before transfection and incubated in 37^0C incubator to reach a 70% confluency. Next day, media was changed one hour before transfection. Transfection mixtures were made according to previously described protocol and incubated for the appropriate time. 10 μL of the transfection mix were added to each well and media was changed 8 hours after transfection. Transfected cells were incubated for 48 hours in 37^0C incubator before adding the MTS dye. 20 μL MTS dye was added in each well and incubated for ~3 hours to monitor the color change by measuring the absorbance at 490 nm. For transfection of PC-3 cells, 3000 cells were seeded in each well and transfected with non-targeting siRNA pool (Dharamfect) and PAINT siRNA pool (Dharmafect). For C4-2B cells, 5000 cells were seeded in individual wells of 96 well plate and transfected with pcDNA3.1+control as a negative control and pcDNA3.1+PAINT as experimental samples.

3.11 Cell Cycle Analysis

Cells were seeded in 6-well plates 24 hours before transfection and transfected as previously described. Media was changed 8 hours after transfection and the cells were further incubated for 48 hours following which they were harvested by trypsinization and collected into complete media. Cells were centrifuged at 840 xg at 4^0C for 5 minutes and washed 3 times with PBS. Washed cells

were collected by centrifugation and resuspended in 300 µL ice-cold 1x PBS. Cells were permeabilized by adding 800 µL of 100% methanol while vortexing samples at low speed and incubating for 30 minutes at -20^{0}C. Next, 5 mL of PBS were added to the fixed cells for rehydration and incubated for 5 minutes on ice. Cells were centrifuged at 840 xg at 4^{0}C for 5 minutes and washed with PBS for 3 times. After final washing, cells were centrifuged and resuspended with 100 µL of 2% BSA (in PBS) containing 100 µg/mL ribonuclease. Cells were incubated for 15 minutes and 300 µL of 2% BSA (in PBS) was added to prevent clumping of cells. Finally, 100 µL of 250µg/mL Propidium Iodide (PI) in 2% BSA (in PBS) was added and incubated for 30 minutes in dark at room temperature. Fluorescent cells were analyzed in Cytoflex S (Beckman Coulter) Flow Cytometer and 10,000 single cells were enumerated with appropriate gating. Cell cycle analysis was performed using FlowJo software by generating histogram and dot plots of samples.

3.12 Migration Assay

Cells were seeded in 24 well plates 24 hours before transfection and transfected as previously described. Media was changed 8 hours after transfection with complete media and incubated for 48 hours before making the scratch. After 48 hours, scratches were made with a 200ul pipette tip and wells were washed 3 times with PBS to remove dislodged cells. Next, fresh media with 5% FBS was added to each well and images were taken which was considered as 0 hour after making the scratch. To continue with the migration assay, cells were incubated in reduced serum media containing 5% FBS at 37^{0}C in a CO_2 incubator and images were taken at 14, 24 and 48 hours after the scratch was made. Analysis of the rate of cell migration were done using ImageJ analysis software.

3.13 Colony Formation Assay

For this assay, cells were seeded on semisolid growth medium and cell growth was monitored by microscopy. Low melting agar (NuSieve) (1%) was melted in a microwave and cooled to 37^0C in a water bath (prepared in hood using autoclaved sterile glassware). Complete media (2x) were warmed at 37^0C and cooled to room temperature for 30 minutes to equilibrate. Next, equal volume of the two solutions were mixed to make a final concentration of 0.5% Agar +1x working media +10% FBS and immediately 1 mL of the mixture was added to each well of a 6-well plate and allowed to incubate at room temperature for 30 minutes to solidify.

After solidifying the base agar, low-melting agarose (NuSieve) (0.6%) was melted in a microwave and cooled to 37^0C in a water bath. At the same time, complete media (2x) was warmed at 37^0C and set aside. Next, trypsinized cells were counted using a hemocytometer after making a single cell suspension. To seed cells, 2 mL of 2x complete media were added to the cell suspension followed by 2 mL of the melted and cooled agarose (0.6%) in a tube and mixed gently by swirling. Next, cell suspension was added to each well (1 mL/well) (5000 cells/well) in 6-well plates. Seeded cells were kept at room temperature for 30-60 minutes to solidify the agarose and incubated at 4^0C for 15 minutes to allow complete solidification. Seeded single cells were incubated at 37^0C incubator for 2 weeks. Cells were supplemented with 0.5 mL complete media every 3 days throughout the incubation time.

After two weeks of incubation, each well was washed with PBS and stained with 0.5 mL of (0.01% Crystal Violet + 10% ethanol in PBS) solution for 2 hours. After staining, each well was washed three times with PBS and incubated overnight at 4^0C. Next day, each well was washed again (2X) with PBS and colonies were visualized with Leica DMi8 microscope and images (5X) were taken

with Leica DFC450C digital camera attached with the microscope. Colonies were counted and grouped based on their diameter as small (<7 um) and large (>7 um). Percentages of small and large colonies were calculated for experimental samples.

3.14 Patient Tissue and Tissue Microarray

Prostate cancer tissue microarray slides with 63 cores of prostate tissues (US Biomax) were used for analysis of PAINT expression in patient tissue samples. Tissue microarray plates had tissue samples from normal prostates and tissue samples of all stages of prostate cancer. Oligonucleotides probes were designed and made by ACD diagnostics and RNA-ISH were performed at the Histology Core Facilities at the University of Florida. Individual images were taken by AperioScope (Leica) and analyzed using QuPath software and expression of PAINT were counted as red dots/100 cells.

3.15 Immunofluorescence assay

C4-2B cells (20000 cells/well) were seeded in 8-well Lab-tek Chamber slides (Thermo Scientific) and incubated for 24 hours before transfection. Cells were transfected with either pcDNA3.1+ control or pcDNA3.1+ PAINT DNA and media was changed 8 hours after transfection. Cells were incubated for 48 hours at 37^0C incubator to perform immunofluorescence assay. Briefly, cells were washed once with PBS and fixed with 4% paraformaldehyde (PFA) in PBS for 20 minutes on ice. Next, PFA was removed and cells were washed twice with 400ul of PBS. Next, 200ul of the permeabilization solution (0.1% Triton X-100) was added and cells were incubated for 30 minutes at room temperature. Cells were washed again with PBS and primary antibodies were added and incubated overnight at 4^0 C.

Next day, the primary antibody solution was removed, and cells were washed with PBS and secondary antibodies were added to each well. Cells were incubated for 30 minutes at room temperature and washed twice with PBS. Phalloidin (25x) stain for actin was added followed by incubation for another 15 minutes at room temperature. Cells were washed twice with PBS. Slides were removed from the chambers and mounted with DAPI Fluoromount-G (Southern Biotech) using coverslips. The prepared slides were imaged using a Leica SP5 confocal microscope and were analyzed with Leica LAS AF software suite. Images were analyzed with Image J software.

3.16 Drug Treatment Assay

Chemotherapeutic agents Docetaxel were used to determine the sensitivity of prostate cancer cells to commonly used drugs upon knockdown of PAINT. PC-3 cells (3000 cells/well) were seeded in individual wells of 96 well plate in 100 μL of complete media. After 24 hours of seeding, PC-3 cells were transfected with siRNAs and media was changed 8 hours after transfection. Drugs were added 24 hours after transfection and incubated again for 48 hours. MTS assays were performed to quantify viable cells at different experimental conditions. PC-3 cells transfected with control siRNA and PAINT siRNA were treated with DMSO as control and treated with different drugs as final concentration of 5 nM and 25 nM Docetaxel (DTX).

3.17 Statistical Analysis

All experiments were repeated with at least 3 or more biological replicates and data were represented as mean ± SD. Student T test were used to analyze statistical significance of all experiments and p value less than 0.05 were used to define significance of all experiments.

CHAPTER FOUR: RESULTS

4.1. Aim 1: Study the Expression Level of PAINT in Prostate Cancer Cells Lines and Tumor Tissues.

In this study, we analyzed transcriptome profiling data to identify differentially expressed mRNAs and lncRNAs in PC-3 subline expressing miR-17-92a compared to PC-3 subline expressing scramble RNA. The top three down-regulated candidate lncRNAs were selected and their expression in cancers were analyzed with in silico based studies. We validated RNA sequencing expression data of our selected long non coding RNA, PAINT, using qRT PCR. Furthermore, we examined expression of PAINT in clinical specimens by RNA in-situ hybridization using prostate Tissue Microarray (TMA) and determined its clinical significance in prostate cancer.

4.1.1 Overexpression of miR-17-92a in PC-3 Cells Dysregulates Several Protein Coding Genes and Long Non-coding RNAs Including PAINT.

Previous study from our lab demonstrates that a subline of PC-3 prostate cancer cells overexpressing miR-17-92a miRNA cluster reduced cell proliferation and cell migration, reduced expression of mesenchymal markers, increased expression of epithelial markers and reduced tumor growth in xenograft mouse models compared to the subline of PC-3 expressing scrambled RNA (93). In this study, we have analyzed transcriptome profiling data from PC-3 subline overexpressing miR-17-92a microRNA cluster compared to the transfected PC-3 cells expressing scrambled RNA. Our analysis revealed that many protein coding genes were dysregulated upon miR-17-92a overexpression (Table 5, 6 and 7) and most of the dysregulated genes are related to cellular and metabolic processes (Figure 6). Furthermore, we observed that not only protein coding genes, but several long non-coding RNAs were also dysregulated in the subline of PC-3 cells

overexpressing miR-17-92a cluster. A majority of the altered lncRNA genes with more than 2 fold change (log_2) in expression and *p* value <0.05 were noted to be located in the exons of protein coding genes either in the sense or antisense orientation (Table 8 and Table 9). Only a small number of lncRNA genes located in the intergenic regions with >2 fold change (log_2) were identified. In this study, we mainly focused on understanding the role of these dysregulated intergenic lncRNAs and selected the top three downregulated lncRNAs for further studies (Table 10). We followed three criteria to determine the top candidates among dysregulated long non-coding RNAs: First, differential expressions of these lncRNAs were at least 2-fold. Second, locations of these lncRNAs were at intergenic positions of the genome. Third, expressions of the lncRNAs were more than 20 FPKM with or without overexpression of the miR-17-92a cluster. Next, in silico analysis was performed to evaluate expression levels of these candidate lncRNAs in different types of cancers. Our analysis revealed that the top most downregulated intergenic lncRNAs, NONHSAT036820 (LINC00888) (PAINT), is upregulated in multiple cancers including colon cancer, melanoma and lung cancer (Table 11) and co-expressed with several tumor suppressors and oncogenes (Table 12).

Table 5: Top 20 up and down regulated protein coding genes upon expression of miR-17-92a in PC-3 cells.

Down regulated protein coding genes	Log_2 (fold change)	Upregulated protein coding genes	Log_2 (fold change)
MSMP	-6.68	S100A9	4.52
AK5	-6.31	CXCL5	4.41
NEFL	-5.53	S100A14	4.00
FGFR1	-5.05	PMEPA1	3.95
VIM	-5.00	LCN2	3.90
CRIP2	-4.88	TMEM135	3.85
IGFBP3	-4.43	CDH1	3.53
MRPS36	-3.47	GRHL2	3.51
COL6A2	-2.77	EFEMP1	3.25
EFNB1	-2.74	ST14	3.18
HRAS	-2.66	C3	3.15
PPAP2B	-2.65	AP1M2	3.11
CDH11	-2.63	FXYD3	3.10
FHL1	-2.60	IL32	3.09
CAPG	-2.47	SEMA6B	3.00
NGRN	-2.45	ESRP1	2.98
RGS2	-2.42	DYSF	2.94
MT-CYB	-2.39	EPHA1	2.93
KCNMA1	-2.32	EPGN	2.86
HOXB13	-2.31	IL6	2.79

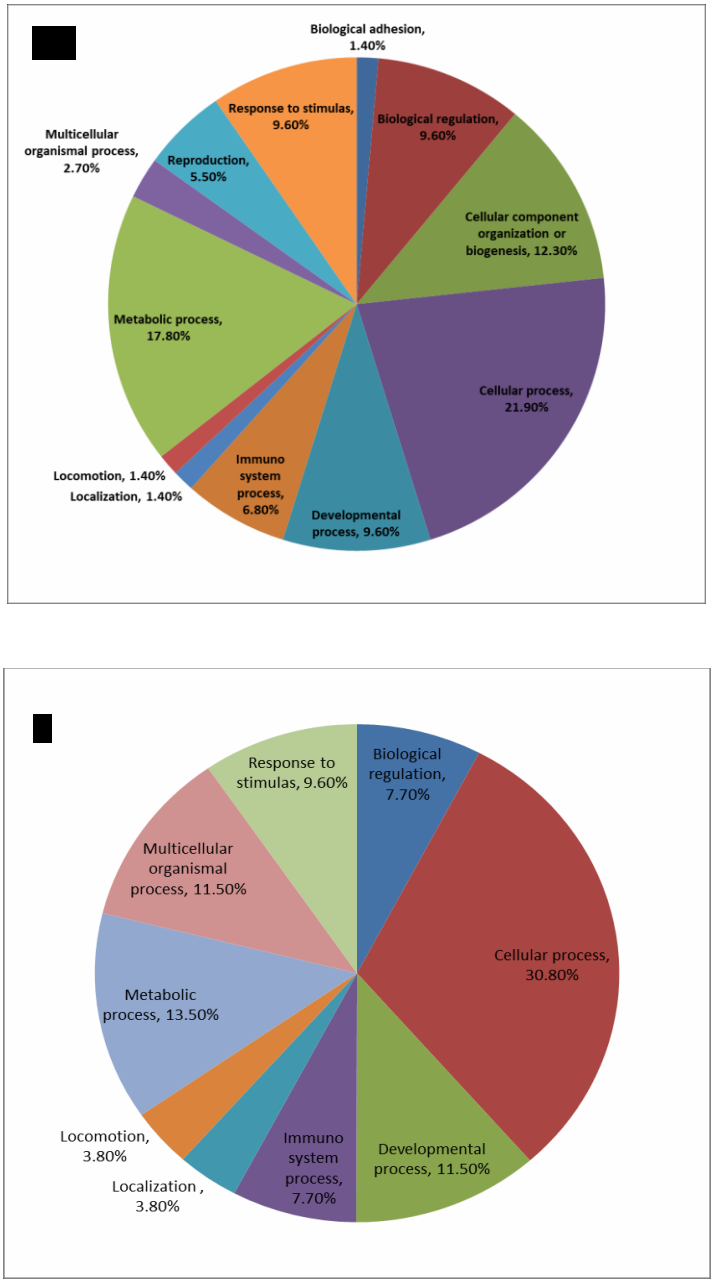

Figure 6: Functional analysis of up and down regulated protein coding genes upon expression of miR-17-92s cluster.

(A) Functional analysis of significantly down-regulated protein coding genes (top). (B) Functional analysis of significantly up regulated protein coding genes (bottom). All differentially expressed genes. $*p < 0.05$.

Table 6: Downregulated cancer-related genes upon expression of miR-17-92a cluster in PC-3 cells.

Cancers (number of related genes)	Down regulated cancer relatedGenes
Lung cancer (7)	HRAS, CSF2, FGFR1, IGFBP3, FHL1, CRIP1, PI3.
Breast cancer (6)	CSF2, FGFR1, HRAS, IGFBP3, AK5, CDH11
Prostate cancer (5)	HOXB13, MSMP, FGFR1, HRAS, IGFBP3

Table 7: Upregulated cancer related genes upon expression of miR-17-92a cluster in PC-3 cells.

Cancers (number of related genes)	Up regulated cancer relatedGenes
Colorectal Cancer (10)	CD44, CDH1, CDH3, CXCL3, EPCAM, LCN2, IL6, TGFB2, THBS1, GAL
Prostate cancer(15)	FXYD3, LCN2, S100A9, CD44, CDH1, CDH3, PTHLH, ST14, TSPAN1, AP1M2, EPCAM, GALNT3, IRF6, PMEPA1, TACSTD2
Breast cancer (10)	CDH1, CD44, CDH3, EPCAM, IL6, KRT7, PTHLH, SEM3A, ST14, MPZL

Table 8: Down regulated long non-coding RNAs dysregulated upon expression of miR-17-92a in PC-3 cells

Transcript ID (NONCODE)	Class	Strand	Log_2 - Fold Change	*p* value	Related gene	Log_2 - Fold Change	*p* value
NONHSAT155167.1	Exonic	Positive	-5.68463	5.00E-05	VIM	-4.9959	5.00E-05
NONHSAT082326.2	Exonic	Negative	-4.97138	0.0253	TFF1	-5.33973	0.2303
NONHSAT216864.1	Exonic	Negative	-4.73294	5.00E-05	NEFL	-5.53166	0.00215
NONHSAT179581.1	Exonic	Negative	-4.31322	0.00015	ZNF91	-7.92489	0.001
NONHSAT069640.2	Exonic	Positive	-3.93034	0.0107	EFR3B	-3.23735	0.00225
NONHSAT189076.1	Exonic	Positive	-3.87323	0.011	PHACTR3	-3.02934	0.00455
NONHSAT026182.2	Exonic	Positive	-3.21617	0.0022	ENO2	-1.88141	0.2128
NONHSAT014102.2	Exonic	Positive	-3.18168	0.0376	ZNF503	-1.942	0.2302
NONHSAT170692.1	Exonic	Positive	-3.13498	0.0077	GCHFR,	N/A	0.0666
NONHSAT047669.2	Exonic	Negative	-3.09879	0.00235	BCL2A1	-2.32538	0.04945
NONHSAT178169.1	Exonic	Negative	-3.05978	0.00355	EPB41L3	-2.70173	0.0007
NONHSAT073124.2	Exonic	Negative	-2.83768	0.02845	SH3RF3	N/A	0.01055
NONHSAT067620.2	Exonic	Negative	-2.74421	0.00075	ZNF160	-2.32	0.00495
NONHSAT201120.1	Intergenic	Positive	-2.68757	0.03545	no gene	N/A	N/A
NONHSAT155720.1	Exonic	Negative	-2.66693	0.00055	KCNMA1	-2.32412	0.0103
NONHSAT157117.1	Exonic	Negative	-2.59999	0.0014	H2AFY2	-2.224	0.0548
NONHSAT223626.1	Exonic	Negative	-2.57256	0.006	CD99L2	-2.42893	0.0034

Table 9: Upregulated long non-coding RNAs upon expression of miR-17-92a in PC-3 cells

Transcript ID (NONCODE)	Class	Strand	Log_2 - Fold change	*p* value	Related mRNA	Log_2 - Fold change	*p* value
NONHSAT200055.1	Exonic	Negative	4.41238	5.00E-05	CXCL5	4.41354	0.00065
NONHSAT096877.2	Exonic	Negative	4.32071	5.00E-05	CXCL5	4.41354	0.00065
NONHSAT220204.1	Exonic	Positive	4.11041	5.00E-05	LCN2	3.8995	5.00E-05
NONHSAT221359.1	Exonic	Negative	4.06654	5.00E-05	LCN2	3.8995	5.00E-05
NONHSAT170674.1	Exonic	Positive	4.02492	0.0002	THBS1	2.23378	0.00405
NONHSAT143306.2	Exonic	Positive	3.43338	5.00E-05	CDH1	3.52832	0.00175
NONHSAT095917.2	intergenic	Negative	3.26831	0.00535	N/A	N/A	N/A
NONHSAT173095.1	Exonic	Positive	3.26093	0.00715	LPCAT2	3.911	0.0077
NONHSAT163558.1	Exonic	Negative	3.24042	0.0026	KRT5	1.21777	1
NONHSAT028744.2	Exonic	Positive	3.16339	0.0042	ERBB3	N/A	N/A
NONHSAT162857.1	Exonic	Positive	3.14315	0.0035	HSPB8	3.55989	0.00775
NONHSAT122221.2	intergenic	Positive	3.14233	0.0052	MYH16	3.44583	1
NONHSAT212733.1	Exonic	Positive	3.04688	0.003	AKR1B10	2.95843	0.03865
NONHSAT086830.2	Exonic	Positive	3.02727	0.00315	FAM83F	1.95398	0.12975
NONHSAT080517.2	Exonic	Positive	2.95277	0.00845	PMEPA1	3.94991	5.00E-05
NONHSAT143305.2	Exonic	Negative	2.95155	0.0139	CDH1	3.52832	0.00175
NONHSAT037680.2	Exonic	Negative	2.92391	0.01325	RBM25	N/A	N/A
NONHSAT138569.2	Exonic	Negative	2.83679	0.0117	MBNL3	N/A	N/A

Transcript ID (NONCODE)	Class	Strand	Log_2 - Fold change	*p* value	Related mRNA	Log_2 - Fold change	*p* value
NONHSAT217374.1	Exonic	Negative	2.78927	0.00095	ESRP1	2.98389	0.001
NONHSAT179375.1	Exonic	Positive	2.77114	0.0136	SEMA6B	2.9953	0.0057
NONHSAT170675.1	Exonic	Positive	2.75895	0.00015	THBS1	2.23378	0.00405
NONHSAT202585.1	Intronic	Positive	2.74541	0.0192	ITGA2	1.41656	0.03405
NONHSAT198720.1	Exonic	Positive	2.69507	0.01385	PARM1	1.88152	1
NONHSAT159006.1	Exonic	Positive	2.6183	0.00705	EHF	2.52827	0.00955
NONHSAT156344.1	Exonic	Positive	2.6048	0.0203	PTPRE	N/A	N/A
NONHSAT115129.2	Exonic	Negative	2.60329	0.01015	MAP7	3.26746	0.04305

Table 10: Top three down regulated intergenic lncRNAs after overexpression of miR-17-92a.

LncRNA ID	Log_2-fold change
A. NONHSAT036820 (LINC00888) (PAINT)	-3.46
B. NONHSAT201120	-2.69
C. NONHSAT221895	-2.00

Table 11: Expression of top three candidate intergenic lncRNAs in different cancers compared to respective normal tissues (EMBL Expression Atlas)

LncRNA ID	Log_2-fold change
A. NONHSAT036820 (PAINT)	PC-3 liver metastasis(mice)(1.9), Colon cancer(2.9,2.6), Breast cancer (2.4), Melanoma (2.3)

Table 12: Co-expression of oncogenes and tumor suppressor genes with PAINT

Gene	Log_2-fold change	Expression in prostate cancer
PAINT (LINC00888)	-3.4	Upregulation
VIM	-4.99	Upregulation
FGFR1	-5.00	Upregulation
CDH1	3.52	Down regulation
CST6	3.25	Down regulation
IRF6	2.25	Down regulation
TACSTD2	2.00	Down regulation
miR-205	3.18	Down regulation

4.1.2 Structure and Expression of PAINT in Different Tissues and Cells

Our expression analysis of the RNA sequencing results revealed that PAINT was downregulated in miR-17-92a expressing PC-3 cells and in silico-based study showed that PAINT lncRNA is differentially expressed in different cancers. These observations provided a strong rationale for focusing our study on the functional characterization of PAINT in prostate cancer. PAINT is an intergenic long non-coding RNA located at positive strand of Chromosome 3 (q27.1) with 8363 genomic length which transcribes 2 isoforms (Genome browser) (Figure 7). We chose the longest isoform consisting of 4 exons with a length 1705 bases and predicted secondary structure containing extensive stems and loops for subsequent expression and functional studies (NONCODE) (Figure 8). GTEx database analysis showed relatively higher expression of PAINT in pituitary (23.74 TPM), adrenal gland (21 TPM) and hypothalamus (18.9 TPM) and low expression in whole blood (0.6 TPM), esophagus mucosa (1.11) and skin (1.27) (GTEx Analysis Release V7). In silico analysis of PAINT expression showed that prostate cancer cell lines that are derived from distant metastasis exhibit higher expressions compared to primary prostate cancer cell lines, cell lines derived from lymph node metastasis and normal prostate cell lines (95) (Figure 9A). Furthermore, we observed that androgen deprivation therapy increased expression of PAINT in androgen sensitive LNCaP prostate cancer cell line (Figure 9B) (96).

Figure 7: PAINT (LINC00888) genomic location and structure. (Source: UCSC Genome Browser on Human Dec. 2013 (GRCh38/hg38) Assembly).

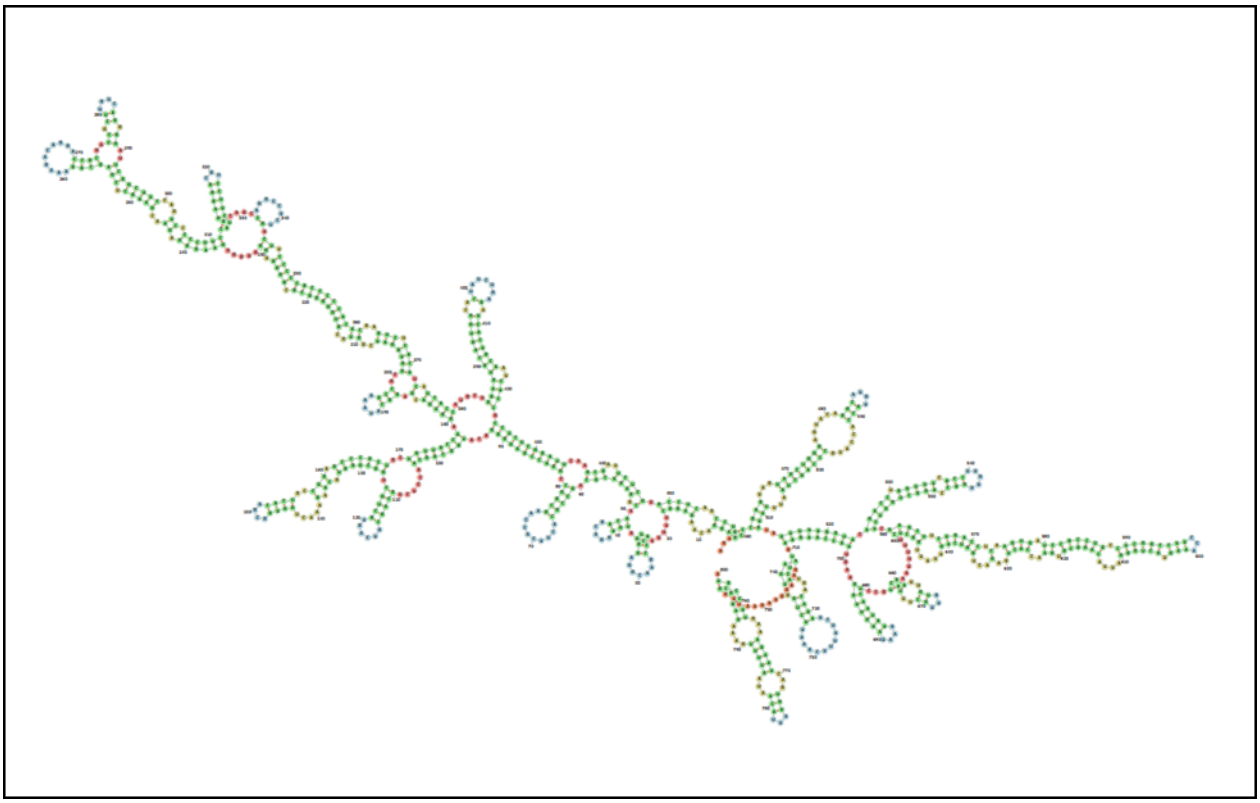

Figure 8: Secondary structure of PAINT

Source: NONCODE (lncRNA database)

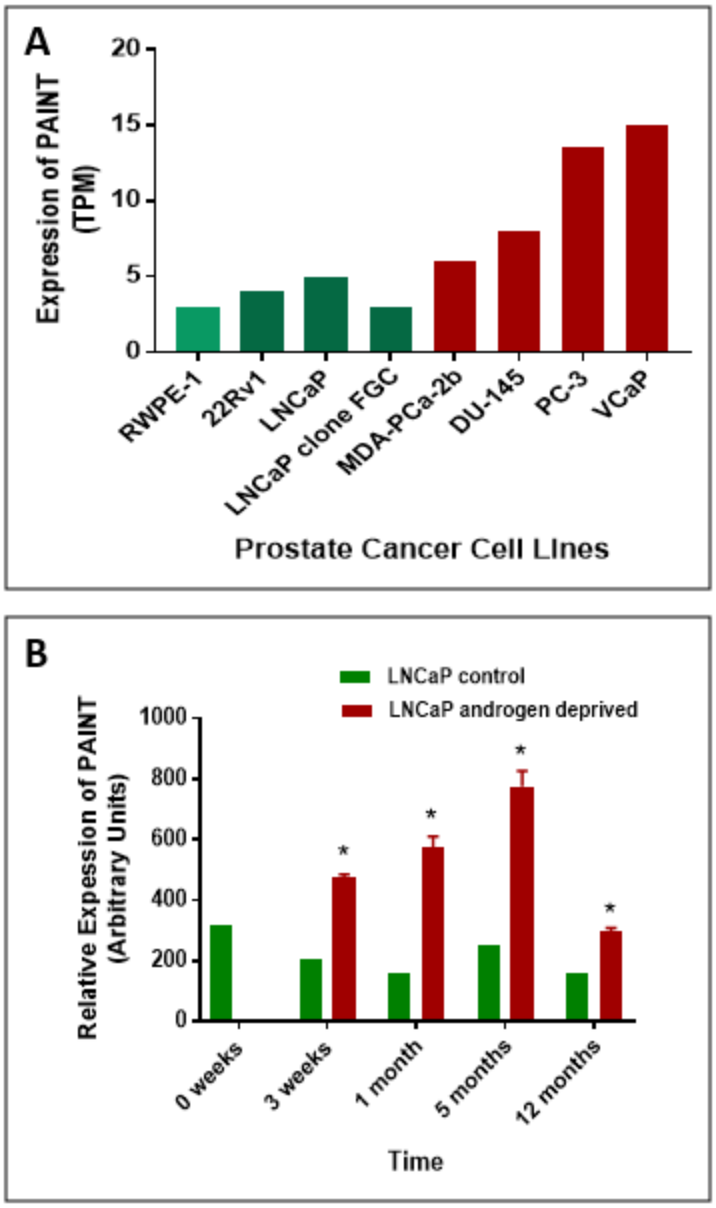

Figure 9: Aggressive prostate cancer cells showed higher expression of PAINT.

(a) Expression of PAINT in prostate cancer cell lines derived from distant metastasis showing higher expressions compared to other prostate cell lines (source: Jordi, et al, 2012). (B) Expression on PAINT in androgen deprived LNCaP cells up to 12 months showing higher expression compared to control LNCaP cells (Source: Monjon et al, 2008). Data show the mean ± SD. *p <0.05.

4.1.3 PAINT Expression were Decreased after Overexpression of miR-17-92a

Transcriptome analysis of PC-3 cells expressing miR-17-92a cluster miRNAs showed that PAINT was down regulated (>3-fold) compared to the cells expressing non-specific RNAs. We performed qRT-PCR based expression analysis of PAINT to validate RNA seq analysis data upon transient transfection of miR-17-92a construct DNA. We transfected PC-3 cells with pLVX-TetOne-Puro inducible vector containing precursor DNA of miR-17-92a cluster miRNAs and pLVX-TetOne-Puro vector containing scrambled RNA. Transfected cells were induced with doxycycline (1 μg/ml) 24 hours after transfection. Expression of all members of miR-17-92a cluster were confirmed by qRT-PCR, which showed an increase between 3 to 9-fold (Figure 10A). Next, we examined the expression of PAINT in these cells. A significant reduction (34% in PAINT expression (figure 10B) was noted in these cells, which further validated the transcriptome profiling data showing downregulation of PAINT upon miR-17-92a overexpression in PC-3 cells.

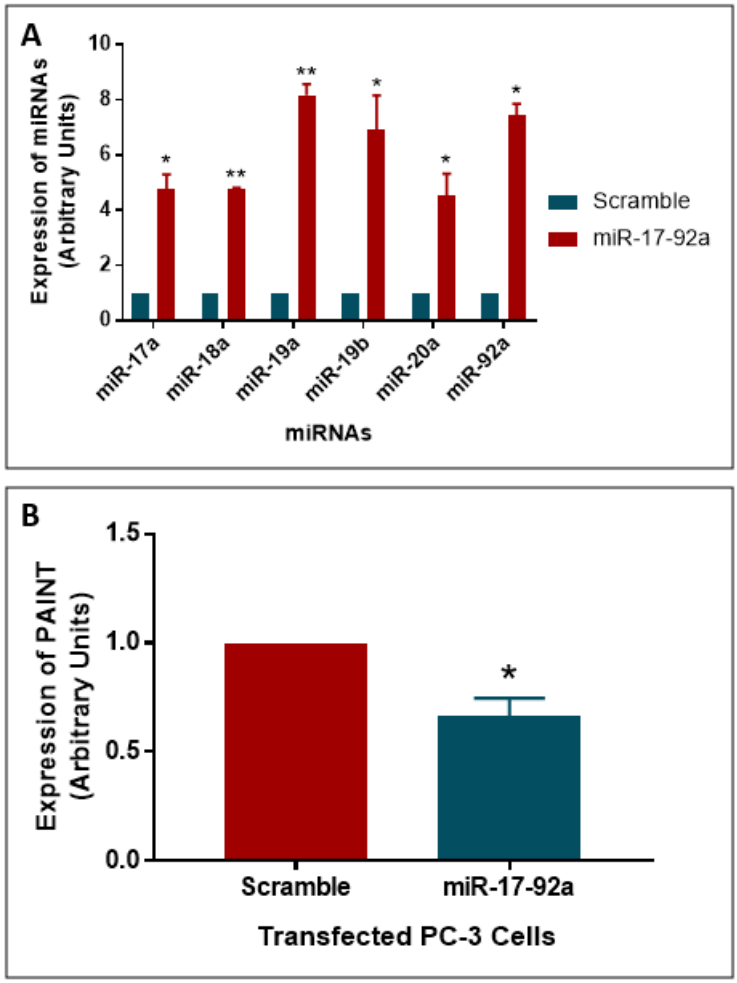

Figure 10: Overexpression of miR-17-92a downregulates PAINT expression in PC-3 cells.

(A) Quantitative RT-PCR analysis of miR-17a, miR-18a, miR-19a, miR-19b, miR-20a and miR-92a showing overexpression of all members of miR-17-92a cluster in miR-17-92a expressing PC-3 cells in comparison with scramble RNA expressing cells after 48 hours of transfection. Three reference genes (RNU43, U1 snRNA and U6 snRNA) were used to normalize raw expression data from qRT-PCR. Data show the mean ± SD. *$p < 0.05$, **$p < 0.005$. (B) Quantitative RT-PCR analysis showing down regulation of PAINT RNA in PC-3 cells at 48 hours after transfection of miR-17-92a compared to PC-3 cells transfected with scrambled RNA. Two reference genes (RPL13A and EIF3D) were used to normalize qRT-PCR C_T values. Data show the mean ± SD. *p =0.018.

4.1.4 PAINT Showed Increased Expression in Aggressive Prostate Tumor Tissues and Prostate Cancer Cell Lines

In silico analysis showed increased expression of PAINT in several cancers (Table 10). In this experiment, we determined endogenous expression of PAINT in different prostate cancer cell lines using qRT-PCR. Our results showed that highly metastatic prostate cancer (distant metastatic) cell lines exhibit higher expression of PAINT compared to other prostate cancer cell lines. (Figure 11A). Furthermore, we studied expression levels of PAINT in prostate tumor tissues using tissue microarrays (US BioMax). The composition of TMAs with specific stages is shown in Table 13. We used PAINT anti-sense oligo probes or non- specific control RNAs (positive controls) for RNA-ISH of the endogenous transcripts in tissue samples. Our analysis showed that PAINT is overexpressed in aggressive/late stage prostate cancer tissues compared to the early stage prostate cancers and in normal prostate tissue samples. We performed RNA-ISH in tissue microarrays consisted of 11 samples of stage IV prostate cancer, 15 samples of stage III prostate cancer, 25 samples of stage II prostate cancer and 3 samples of normal prostate tissues. Analysis of RNA-ISH images revealed that PAINT was distinctly upregulated in stage II, stage III and stage IV compared to normal prostate tissues (Figure 11B and 12). We also noted higher expression of PAINT in stage III and stage IV prostate cancer tissues compared to stage II tissues (Figure 11B and 12). These studies clearly indicate that PAINT is upregulated in highly aggressive prostate cancer tissues and cell lines and suggest its potential involvement in aggressive prostate cancer.

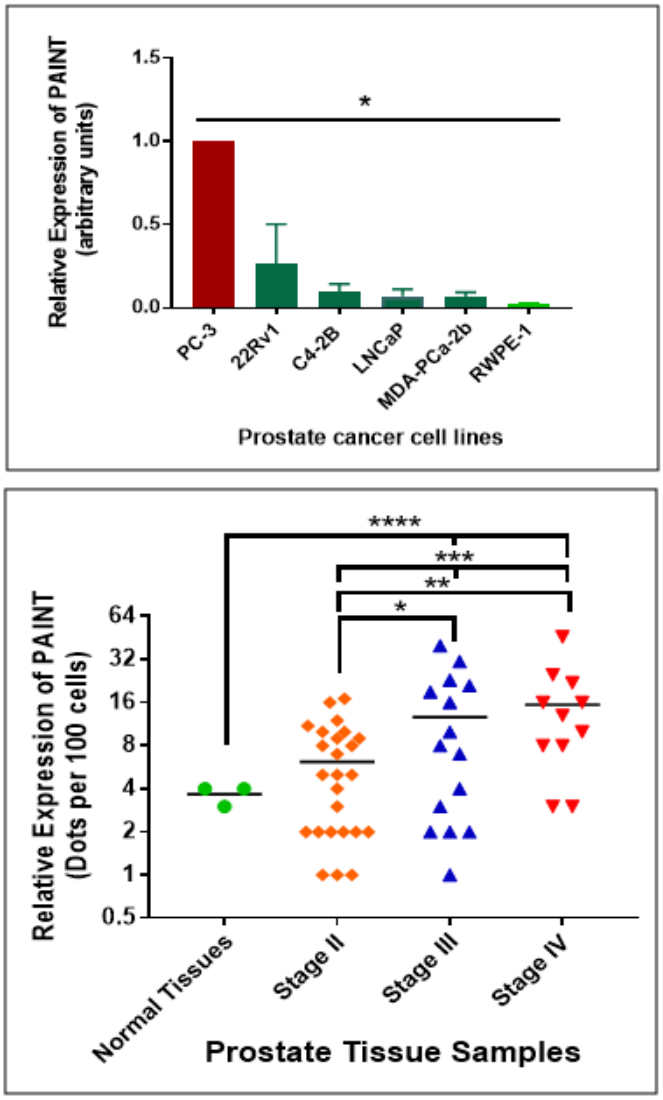

Figure 11: PAINT shows increased expression in aggressive prostate cancer tissues and metastatic prostate cancer lines

(A) Expression of PAINT in prostate cancer cell lines. qRT-PCR based expression analysis results showing highest expression of PAINT in bone metastatic PC-3 cells. Data was represented as mean ± SD. *$p < 0.0001$. (B) Comparative analysis of expression of PAINT in prostate cancer tissues. RNA-ISH performed using prostate tissue microarray with 54 cores (N=3, stage II = 25, stage III = 15, stage IV = 11) to determine expression of PAINT in different stages of prostate cancer and normal tissues. *p=0.02, **p=0.0022, ***p=0.013, ****p=0.016.

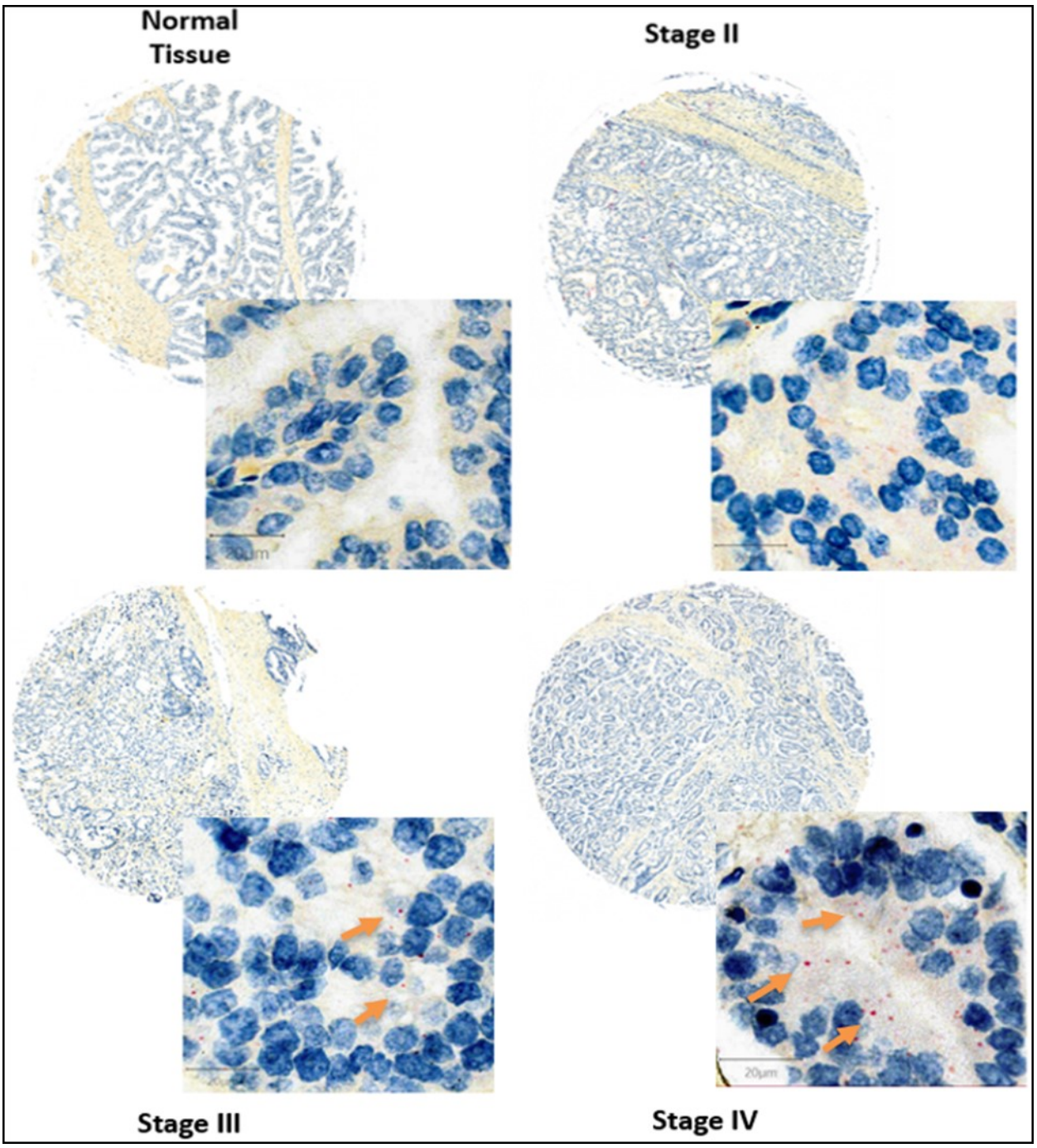

Figure 12: Representative tissue microarray (TMA) images of RNA in-situ hybridization of PAINT in tissues from normal prostate and different stages of prostate cancer. Left-top, right-top, left-bottom, right-bottom images are representative RNA-ISH images of Normal, stage II, stage III and stage IV prostate cancer tissues. Arrows showing positive signals (Red dots).

Table 13: Characteristics of prostate cancer patient tissues in tissue microarray.

No.	Age	Sex	Organ/ Anatomic Site	Pathology diagnosis	TNM	Grade	Stage	Type	Tissue ID.	Gleason Score	Gleason Grade
1	71	M	Prostate	Adenocarcinoma	T2N0M0	1	II	malignant	Mpr080049	1+2	2
2	60	M	Prostate	Adenocarcinoma (sparse)	T3aN0M0	1	III	malignant	Mpr080010	2+2	2
3	66	M	Prostate	Adenocarcinoma	T3N1M1	1	IV	malignant	Mpr020491	1+2	2
4	71	M	Prostate	Adenocarcinoma	T1N0M0	1	I	malignant	Mpr080053	2+2	2
5	71	M	Prostate	Adenocarcinoma	T2N0M0	1	II	malignant	Mpr070077	1+2	2
6	76	M	Prostate	Adenocarcinoma	T2aN0M0	1	II	malignant	Mpr040106	2+2	2
7	72	M	Prostate	Adenocarcinoma	T2N0M0	1	II	malignant	Mpr040048	1+2	2
8	73	M	Prostate	Adenocarcinoma	T3N0M0	1	III	malignant	Mpr090005	2+2	2
9	71	M	Prostate	Adenocarcinoma	T2N0M0	2	II	malignant	Mpr080033	2+3	3
10	74	M	Prostate	Adenocarcinoma	T4N1M1	1	IV	malignant	Mpr040041	2+2	2
11	75	M	Prostate	Adenocarcinoma	T2N0M0	2	II	malignant	Mpr030207	2+4	3
12	69	M	Prostate	Adenocarcinoma (sparse)	T2N0M0	1	II	malignant	Mpr020114	1+2	2
13	78	M	Prostate	Adenocarcinoma	T3N2M1	2	IV	malignant	Mpr010048	2+4	3
14	73	M	Prostate	Adenocarcinoma	T2N0M0	2	II	malignant	Mpr050122	3+3	3
15	65	M	Prostate	Adenocarcinoma	T2N0M0	2	II	malignant	Mpr030031	3+3	3
16	73	M	Prostate	Adenocarcinoma (cataplasia tissue)	T2N0M0	-	II	malignant	Mpr070068	-	-
17	70	M	Prostate	Adenocarcinoma	T2N1M1c	2	IV	malignant	Mpr020345	3+3	3
18	58	M	Prostate	Adenocarcinoma	T2N0M0	2	II	malignant	Mpr050125	3+3	3
19	64	M	Prostate	Adenocarcinoma	T2aN0M0	2	II	malignant	Mpr040171	3+3	3

No.	Age	Sex	Organ/ Anatomic Site	Pathology diagnosis	TNM	Grade	Stage	Type	Tissue ID.	Gleason Score	Gleason Grade
20	62	M	Prostate	Adenocarcinoma	T2N0M0	2	II	malignant	Mpr050083	3+3	3
21	60	M	Prostate	Adenocarcinoma	T3N1M0	2	IV	malignant	Mpr080011	2+4	3
22	65	M	Prostate	Adenocarcinoma	T2N0M0	2	II	malignant	Mpr070087	3+3	3
23	82	M	Prostate	Adenocarcinoma	T3N0M0	1	III	malignant	Mpr040075	2+2	2
24	64	M	Prostate	Adenocarcinoma	T2N0M0	2	II	malignant	Mpr060077	2+4	3
25	65	M	Prostate	Adenocarcinoma	T2N0M0	2	II	malignant	Mpr040034	3+3	3
26	73	M	Prostate	Adenocarcinoma	T3N1M0	2	IV	malignant	Mpr030433	3+3	3
27	70	M	Prostate	Adenocarcinoma	T2N0M0	3	II	malignant	Mpr020038	4+4	4
28	72	M	Prostate	Adenocarcinoma	T3N0M0	3	III	malignant	Mpr050093	4+5	4
29	26	M	Prostate	Adenocarcinoma	T2N0M0	3	II	malignant	Mpr060006	4+4	4
30	62	M	Prostate	Adenocarcinoma	T3N0M0	2--3	III	malignant	Mpr040089	4+3	3--4
31	64	M	Prostate	Adenocarcinoma	T2N0M0	2	II	malignant	Mpr070118	3+3	3
32	64	M	Prostate	Adenocarcinoma	T3N0M0	2	III	malignant	Mpr020003	2+4	3
33	69	M	Prostate	Adenocarcinoma	T3N0M0	2	III	malignant	Mpr030166	2+4	3
34	51	M	Prostate	Adenocarcinoma	T2N0M0	3	II	malignant	Mpr050073	4+5	4
35	73	M	Prostate	Adenocarcinoma	T3N0M0	3	III	malignant	Mpr030374	4+5	4
36	78	M	Prostate	Adenocarcinoma	T4N1M1b	2	IV	malignant	Mpr030228	3+4	3
37	20	M	Prostate	Adenocarcinoma	T3N0M0	2	III	malignant	Mpr060171	3+4	3
38	66	M	Prostate	Adenocarcinoma	T3aN0M0	2--3	III	malignant	Mpr060047	4+3	4
39	80	M	Prostate	Adenocarcinoma	T3N0M0	2	III	malignant	Mpr020382	3+3	3

No.	Age	Sex	Organ/ Anatomic Site	Pathology diagnosis	TNM	Grade	Stage	Type	Tissue ID.	Gleason Score	Gleason Grade
40	70	M	Prostate	Adenocarcinoma (smooth muscle)	T3N0M0	-	III	malignant	Mpr060100	-	-
41	81	M	Prostate	Adenocarcinoma	T3N0M0	3	III	malignant	Mpr020317	4+5	5
42	61	M	Prostate	Adenocarcinoma	T3N1M0	3	IV	malignant	Mpr070019	4+5	5
43	40	M	Prostate	Adenocarcinoma (hyperplasia)	T2N0M0	-	II	malignant	Mpr030239	-	-
44	76	M	Prostate	Adenocarcinoma (hyperplasia)	T3N0M0	-	III	malignant	Mpr020387	-	-
45	64	M	Prostate	Adenocarcinoma	T2N0M0	3	II	malignant	Mpr040194	4+5	4
46	69	M	Prostate	Adenocarcinoma	T2N0M0	2	II	malignant	Mpr030352	3+5	3
47	62	M	Prostate	Adenocarcinoma	T2N0M0	3	II	malignant	Mpr040163	4+4	4
48	82	M	Prostate	Adenocarcinoma	T2N0M0	3	II	malignant	Mpr030147	4+4	4
49	75	M	Prostate	Adenocarcinoma	T2N0M0	3	II	malignant	Mpr030402	5+4	5
50	73	M	Prostate	Adenocarcinoma	T4N0M0	3	IV	malignant	Mpr030188	5+4	5
51	67	M	Prostate	Adenocarcinoma	T2N0M0	3	II	malignant	Mpr040165	5+4	5
52	75	M	Prostate	Adenocarcinoma	T3N1M0	3	IV	malignant	Mpr020157	5+5	5
53	60	M	Prostate	Adenocarcinoma	T2N0M0	3	II	malignant	Mpr020323	5+5	5
54	60	M	Prostate	Adenocarcinoma	T3N1M0	3	IV	malignant	Mpr030236	5+4	5
55	63	M	Prostate	Adenocarcinoma	T2N0M0	3	II	malignant	Mpr030347	5+4	5
56	56	M	Prostate	Adenocarcinoma	T2N0M0	3	II	malignant	Mpr040206	5+5	5
57	76	M	Prostate	Adenocarcinoma	T2aN0M0	3	II	malignant	Mpr030277	4+4	4

No.	Age	Sex	Organ/ Anatomic Site	Pathology diagnosis	TNM	Grade	Stage	Type	Tissue ID.	Gleason Score	Gleason Grade
58	77	M	Prostate	Adenocarcinoma	T2N0M0	3	II	malignant	Mpr040215	5+4	5
59	75	M	Prostate	Adenocarcinoma	T3N0M0	3	III	malignant	Mpr040214	5+5	5
60	66	M	Prostate	Adenocarcinoma	T2N0M0	3	II	malignant	Mpr020016	5+5	5
61	36	M	Prostate	Normal prostate tissue		-		normal	Mpr11N013	-	-
62	37	M	Prostate	Normal prostate tissue	-	-	-	normal	Mpr07N028	-	-
63	31	M	Prostate	Normal prostate tissue	-	-	-	normal	Mpr11N008	-	-

4.2 Aim 2. Examine the Function of PAINT in Prostate Cancer Cells.

In this aim, we examined the functions of PAINT in prostate cancer cells using both silencing and overexpression studies. We selected PC-3 cells as an in-vitro model for silencing studies because it showed higher expression of PAINT compared to other prostate cancer cells. C4-2B cells were used for overexpression studies because these cells express low amounts of PAINT. Here, we evaluated the involvement of PAINT in prostate cancer cell phenotypes through studies such as cell proliferation, cell cycle progression, cell migration, colony formation and expression of markers involved in these properties.

4.2.1 Silencing of PAINT Inhibits Aggressive Prostate Cancer Phenotypes

4.2.1.1 Silencing of PAINT Changed Cell Morphologies.

Expression analysis of PAINT in prostate cancer tissues and cell lines demonstrated that PAINT is highly expressed in aggressive prostate cancer tissues and metastatic prostate cancer cell lines suggesting its potential involvement in progression of prostate cancer. To explore the mechanistic functions of PAINT in prostate cancer, we silenced PAINT expression in PC-3 cells through transfection of PAINT siRNAs. Transient transfection of PC-3 cells with PAINT siRNA showed ~ 80% reduction in expression compared to cells transfected with non-targeting siRNA (figure 13A) as monitored by qRT-PCR. Knockdown of PAINT changed PC-3 cells morphology from its parental spindle shape to a cuboidal shape (Figure 13B). The change in cell morphology suggests that PAINT is involved in regulation of PC-3 cell structure and other properties.

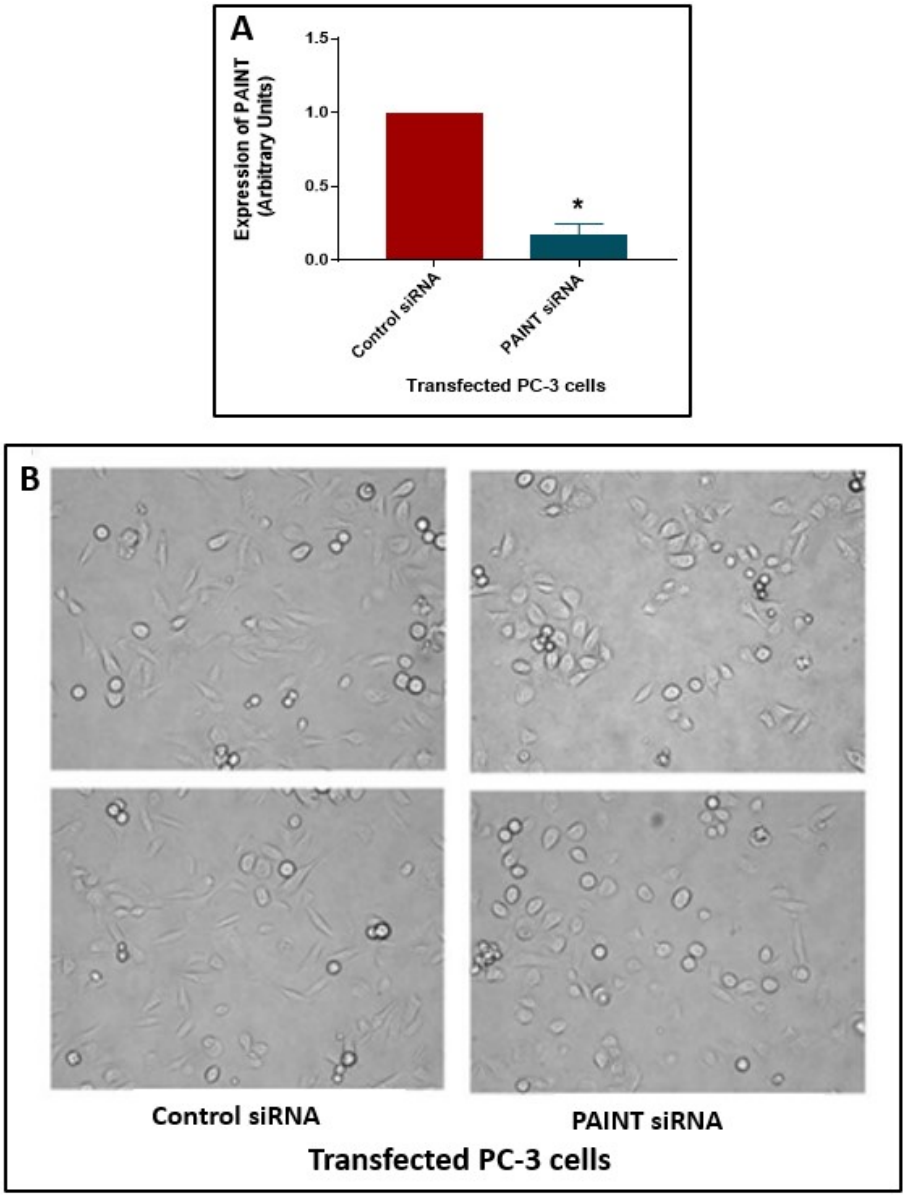

Figure 13: Silencing of PAINT altered PC-3 cell morphology.

A) Quantitative RT-PCR of PAINT transcript in PC-3 cells transfected with PAINT siRNAs showing ~80% down regulation of PAINT compared to non-targeting siRNA. Data represent the mean ± SD of three individual experiments. *$p < 0.05$. (B) Light microscopic images of PC-3 cells transfected with PAINT siRNAs and non-targeting siRNA. PAINT siRNA transfected PC-3 cells showed altered PC-3 morphologies (right panel of images), whereas control siRNA transfected cells showed parental PC-3 cell morphologies (left panel of images).

4.2.1.2 Silencing of PAINT Reduced Cell Proliferation and Activated Pro-apoptosis Markers in PC-3 Cells

We examined the effect of PAINT silencing on PC-3 cell proliferation. MTS chromogenic assays were performed using PAINT siRNA transfected PC-3 cells after 48 of transfection. Our analysis showed that proliferation of PC-3 cells was significantly reduced (26%) after silencing of PAINT compared to non-targeting siRNAs control (Figure 14A). This observation indicates that silencing of PAINT has antiproliferative effects on PC-3 cells.

Next, we examined the involvement of PAINT in preventing apoptosis. We monitored expression of the pro-apoptotic proteins such as activated PARP and Caspase 3 in PC-3 cells upon silencing of PAINT using Western blot analysis. Our results showed that silencing of PAINT significantly activated PARP (Figure 14B and 14C) and Caspase 3 (Figure 14D and 14E) through increased expression of cleaved PARP and Caspase 3 compared to that noted upon transfection of non-specific RNA in PC-3 cells. These results clearly suggest that silencing of PAINT induces apoptosis by activating pro-apoptotic proteins PARP and Caspase-3 in PC-3 cells.

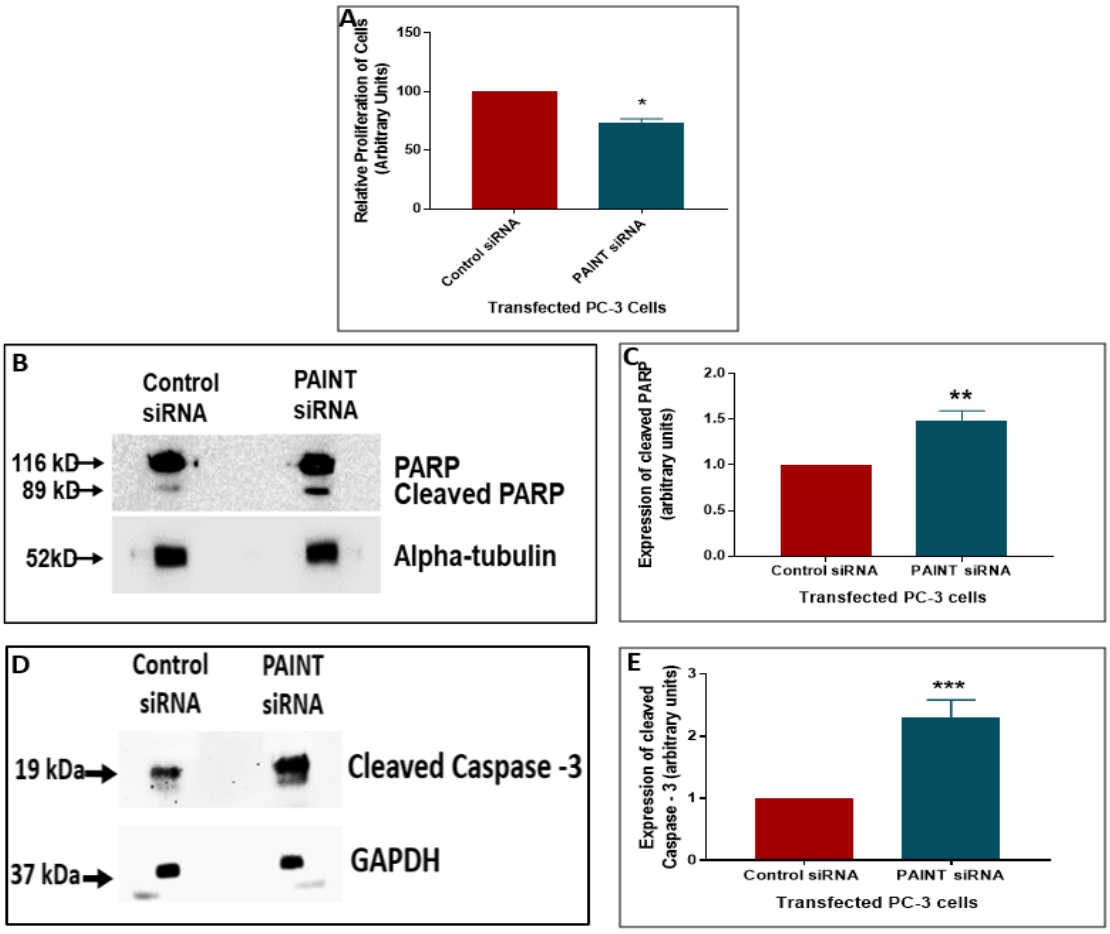

Figure 14: Silencing of PAINT reduced cell proliferation and activated pro apoptotic protein PARP and Caspase-3.

(A) Proliferation of PC-3 cell after knockdown of PAINT. Knock down of PAINT reduced (~ 26%) proliferation of PC-3 cells compared to control PC-3 cells. B) Representative Western blot images of PARP and activated PARP after knocking down of PAINT. C) Densitometric analysis of expression of activated PARP showing 50% increase after silencing of PAINT in PC-3 cells compared to control PC-3 cells. (D) Representative Western blot image of cleaved Caspase -3 upon silencing of PAINT in PC-3 cells. (E) Densitometric analysis cleaved Caspase -3 showing 130% increase after silencing of PAINT in PC-3 cells. (A, C, E) Data show the mean ± SD of three individual experiments. *$p = 0.004$, **$p = 0.016$, ***$p = 0.045$.

4.2.1.3 Silencing of PAINT Inhibit Cell Cycle Progression

Next, we examined the involvement of PAINT in cell cycle progression using PC-3 cells. Cell cycle analysis with PI staining was done with or without silencing of PAINT. Transfected PC-3 cells were harvested at 48 hours after transfection and stained with PI for cell cycle analysis. Our analysis showed ~26% reduction of S phase population of PC-3 cells transfected with PAINT siRNAs compared to PC-3 cells transfected with non-specific RNAs (Figure 15A and 15B). This data indicates that PAINT is possibly involved in cell cycle progression, more specifically in S phase regulation. Altogether, our data showed that silencing of PAINT in PC-3 cells reduced cell proliferation and population of cells in S phase and activated pro-apoptotic proteins PARP and Caspase 3.

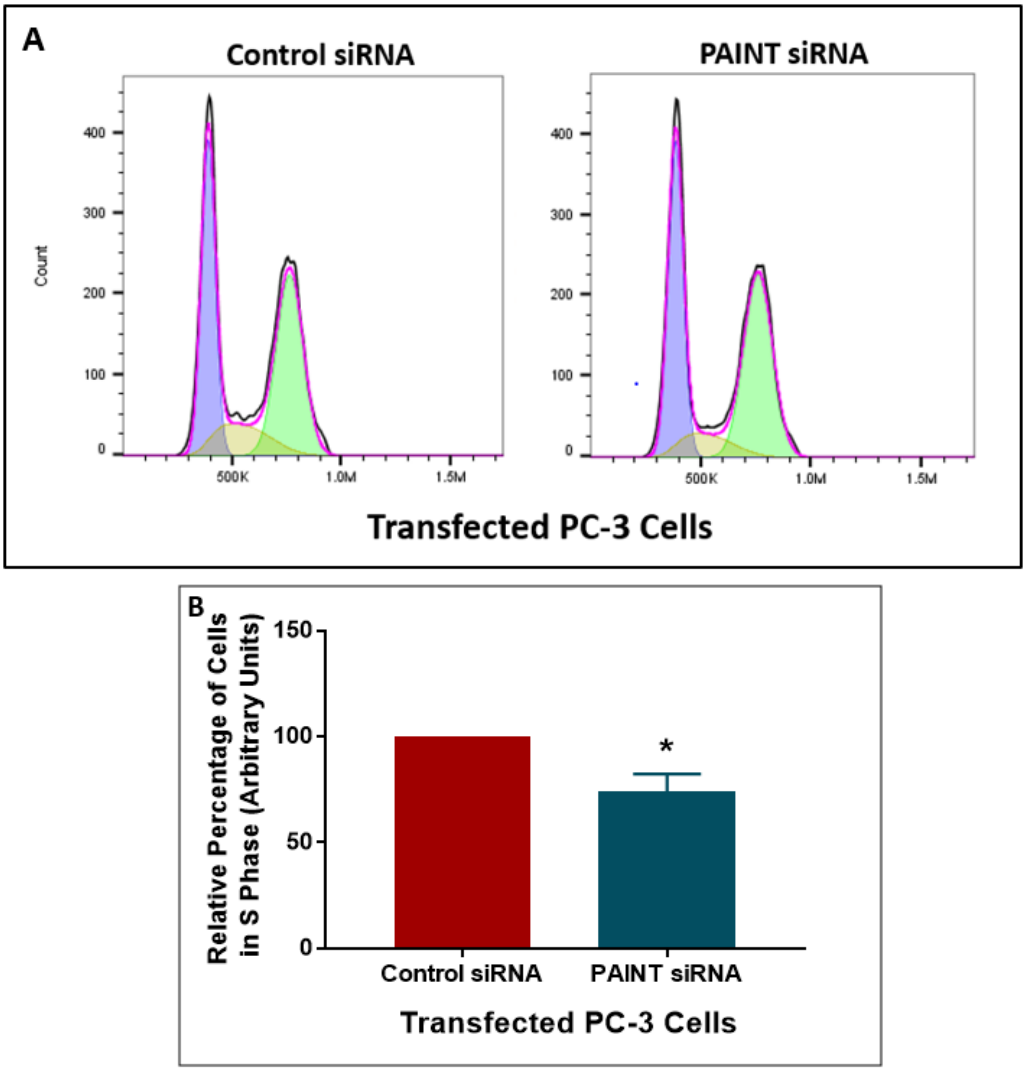

Figure 15: Silencing of PAINT reduced cell cycle progression in PC-3 cells.

(A) Two parameter histogram of cell cycle progression of PI stained PC-3 cells transfected with PAINT siRNAs (left) and non-targeting RNAs (right). (B) Comparative analysis of percentage of cells in S phase showed 26% reduction in S phase population of PC-3 cells upon silencing of PAINT compared to control PC-3 cells. Data represent the mean ± SD of 4 individual experiments. *$p = 0.008$.

4.2.1.4 Silencing of PAINT Inhibited Cell Migration and Altered Expression of Markers for Epithelial Mesenchymal Transition

Previously, we observed that silencing of PAINT changed morphology of PC-3 cells. Here, we intended to evaluate the involvement of PAINT in cell migration. Scratch assays were performed using PC-3 cells transfected with PAINT siRNAs and control RNAs. Analysis of the rate of migration of PC-3 cells after 14 hours of making the scratches showed ~33% reduction in the rate of cell migration compared to the transfected control PC-3 cells (Figure 16A and 16B). This result indicates that PAINT expression is a contributing factor for PC-3 cell migration.

To understand the involvement of canonical protein factors associated with cell migration and EMT in PAINT-mediated cell migration, we examined the expression of the mesenchymal markers Slug and Vimentin and the epithelial marker E-cadherin. Western blot analysis showed significant down regulation in the expression of Slug (57%) (Figure 17A and 17B) and Vimentin (87%) (Figure 17C and 17), but increased expression of E-cadherin (39%) (Figure 17E and 17F). These observations indicate that PAINT is possibly involved in regulation of genes involved in EMT and contributes to the EMT process and migration.

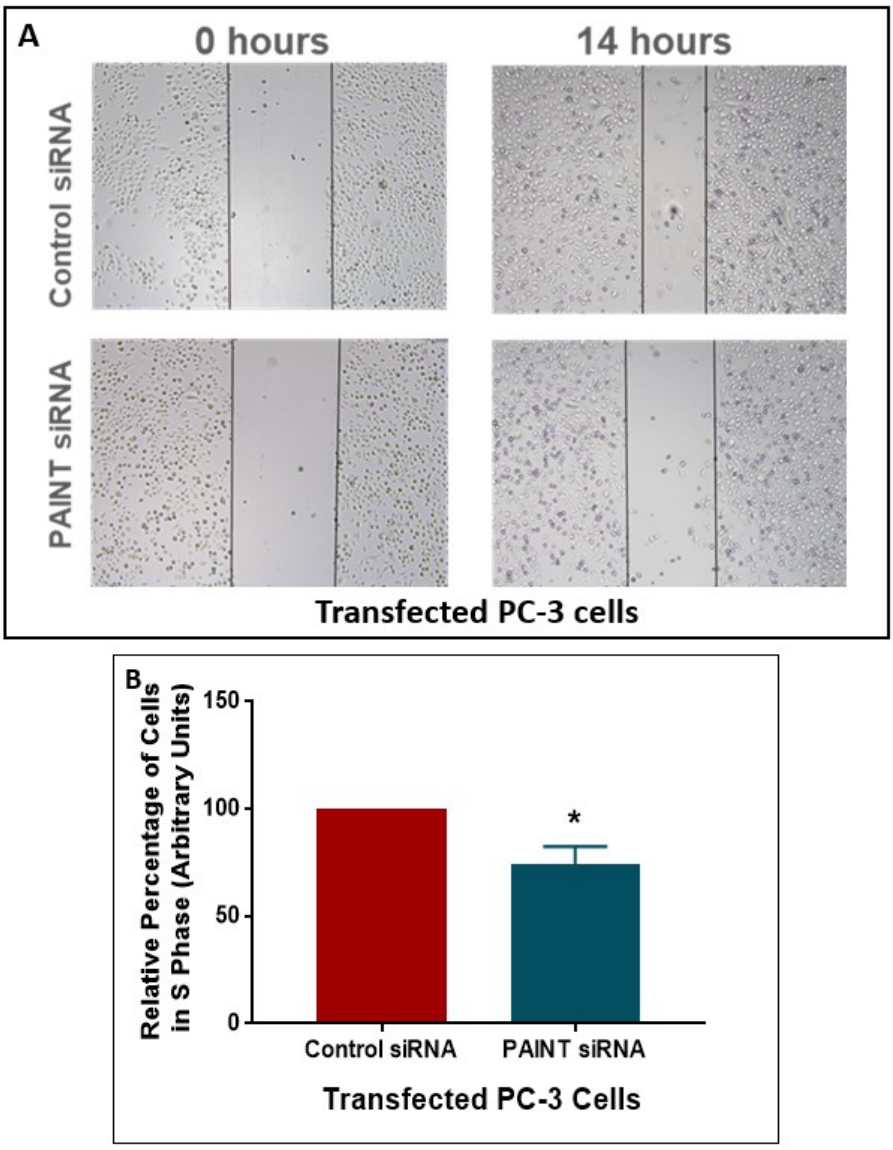

Figure 16: Silencing of PAINT reduced migration of PC-3 cells

(A) Representative images of migration of PC-3 cells transfected with PAINT siRNAs or non-specific RNAs at 0 hours and 14 hours after making the scratch. (B) Analysis of the rate of migration of PC-3 cells showing reduced (33%) migration of PC-3 cells after silencing of PAINT compared to control PC-3 cells. Data show the mean ± SD of three independent experiments. *p = 0.046.

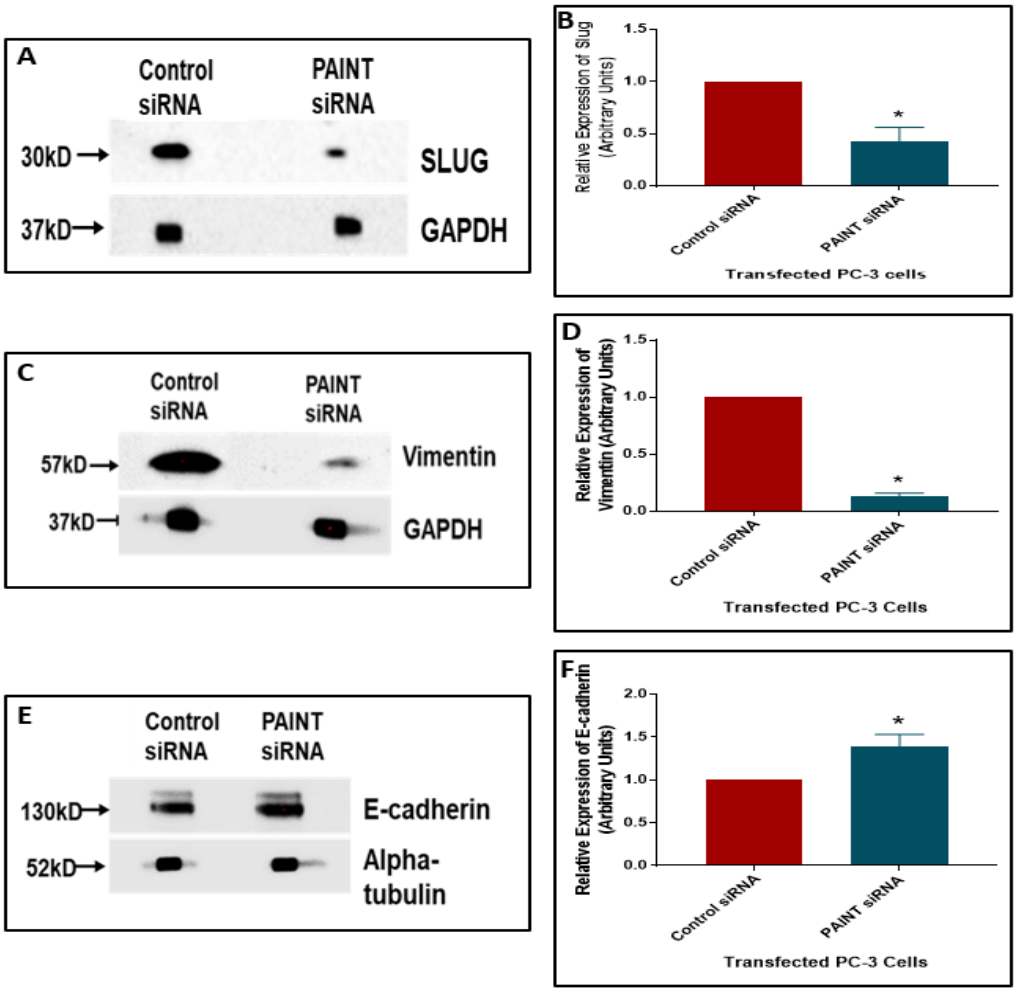

Figure 17: Silencing of PAINT reduced expression of mesenchymal markers and enhanced expression of an epithelial marker.

(A, C, E) Representative Western blot images showing expression of Slug, Vimentin and E-cadherin in PC-3 cell lysates. Silencing of PAINT in PC-3 cells showed reduction of mesenchymal markers Slug and Vimentin, and increased expression of E-cadherin compared to control siRNA transfected PC-3 cells. (B, D, F) Densitometry of Slug, Vimentin and E-cadherin in PC-3 cells transfected with PAINT siRNA and control siRNA. Silencing of PAINT reduced expression of mesenchymal markers Slug and Vimentin by 57% and 87% respectively, and increased expression of E-cadherin by 39%. Data show the mean ± SD of three biological replicates. *$p = 0.018$, **$p = 0.0002$, ***$p = 0.011$.

4.2.1.5 Silencing of PAINT Improves Drug Sensitivity of Aggressive Prostate Cancer Cells

Our earlier experiments involving silencing of PAINT in PC-3 cells suggested its involvement in cell proliferation, cell cycle progression and cell survival. In this study, we examined the beneficial effects of PAINT silencing in improving sensitivity of PC-3 cells to chemotherapeutic agent Docetaxel (DTX) and selective Aurora Kinase Inhibitor VX-680. PC-3 cells were transfected with PAINT siRNAs or control RNAs and treated with chemotherapeutic agent Docetaxel (DTX) and VX-680. Silencing of PAINT increased sensitivity of PC- 3 cells to DTX. DTX treatment with final concentrations of 5nM and 25nM showed 19% and 20% additional reduction in the cell proliferation of PAINT siRNA transfected PC-3 cells compared to non-targeting RNA transfected PC-3 cells (Figure 18A). However, drug sensitivity was not increased when concentration of DTX was increased from 5nM to 25nM (Figure 18A). Furthermore, Silencing of PAINT increased sensitivity to VX-680 about 10% of PC-3 cells. These findings suggest that silencing of PAINT would be a promising therapeutic approach as a combination therapy with chemotherapeutic agent Docetaxel or Aurora kinase inhibitor VX-680 in the treatment of aggressive prostate cancer.

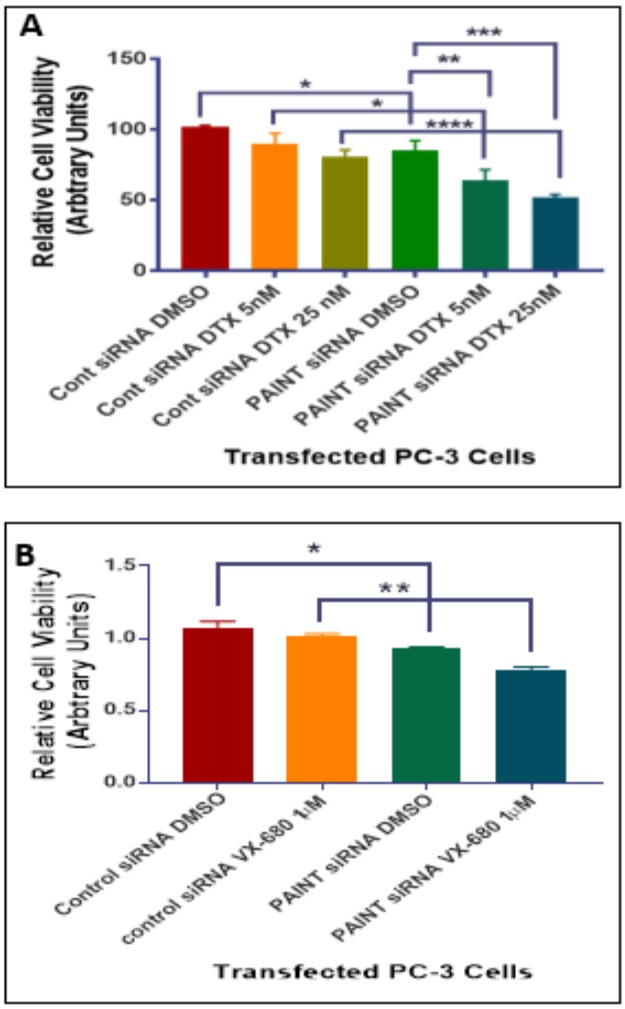

Figure 18: Silencing of PAINT increased sensitivity to chemotherapeutic agent DTX and selective Aurora kinase inhibitor VX-680.

(A) Viability of PC-3 cells transfected with PAINT siRNAs and non-targeting RNAs in combination with DTX or DMSO. Silencing of PAINT in PC-3 cells showed higher sensitivity to DTX (5 nM and 25 nM) treatments compared to DMSO treated PC-3 cells. Data shows the mean ± SD of three individual experiments. *p =0.015, **p=0.022, ***p = 0.001, ****p = 0.0005. (B) Silencing of PAINT in PC-3 cells showed higher sensitivity to selective Aurora Kinase Inhibitor VX-680 1 µM treatments compared to DMSO treated PC-3 cells. Data shows the mean ± SD of three individual experiments. *p =0.014, ** p = 0.0002.

4.2.2 Overexpression of PAINT Promotes Prostate Cancer Progression

4.2.2.1 Overexpression of PAINT Increased Cell Proliferation in C4-2B Cells

Earlier studies showed that silencing of PAINT in PC-3 cells reduced cell proliferation, reduced cell cycle progression and enhanced the activation of pro-apoptotic markers. In this experiment, we generated stable subline of C4-2B cells by transfecting with pcDNA 3.1+ empty vector and pcDNA3.1+PAINT cDNA of the spliced transcript (1.7 kB). We chose C4-2B cells because of its less aggressiveness compared to PC-3 cells and lower expression of PAINT. Antibiotic resistant colonies were isolated, cloned and the level of PAINT expression in each clone was determined by quantitative RT-PCR. Analysis of PAINT expression showed 6.1-fold upregulation of PAINT compared to the control C4-2B subline in several colonies which are pooled together to generate the C4-2B transfected subline (Figure 19A).

Next, we examined proliferation of C4-2B cells overexpressing PAINT using MTS colorimetric assays. C4-2B cells overexpressing PAINT showed a 52% higher rate of proliferation compared to control C4-2B cells (Figure 19B). This result suggests that ectopic expression of PAINT promotes cell proliferation.

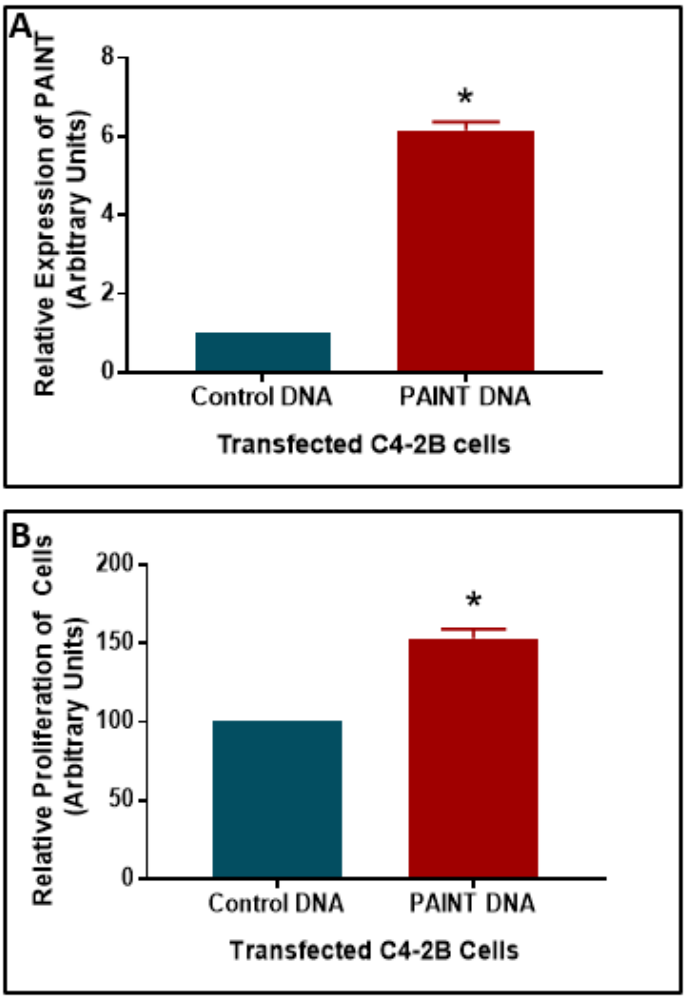

Figure 19: Overexpression of PAINT increased cell proliferation of C4-2B prostate cancer cell line.

(A) Quantitative RT-PCR of PAINT in C4-2B cells showing 6.1-fold upregulation of PAINT compared to control C4-2B subline. Data represent the mean ± SD of three independent experiments. *p = 0.018. (B) MTS assays showing increased cell proliferation (53%) upon expression of PAINT in C4-2B stable subline compared to empty vector DNA expressing control cells. MTS cell proliferation assay were performed 48 hours after seeding. Data represent the mean ± SD of three independent experiments in triplicates. *p = 0.004.

4.2.2.2 Overexpression of PAINT Enhances S-phase Progression in Prostate Cancer Cells.

Next, we studied the effect of expression of PAINT on cell cycle progression. C4-2B stable sublines overexpressing PAINT and control subline were stained with PI and analyzed by flow cytometry. Cell cycle analysis showed an increase (19%) in S-phase cell population in C4-2B subline overexpressing PAINT compared to C4-2B control cells (Figure 20A and 20B). This observation suggests that PAINT expression has a positive effect on S-phase progression which leads to increased cell proliferation.

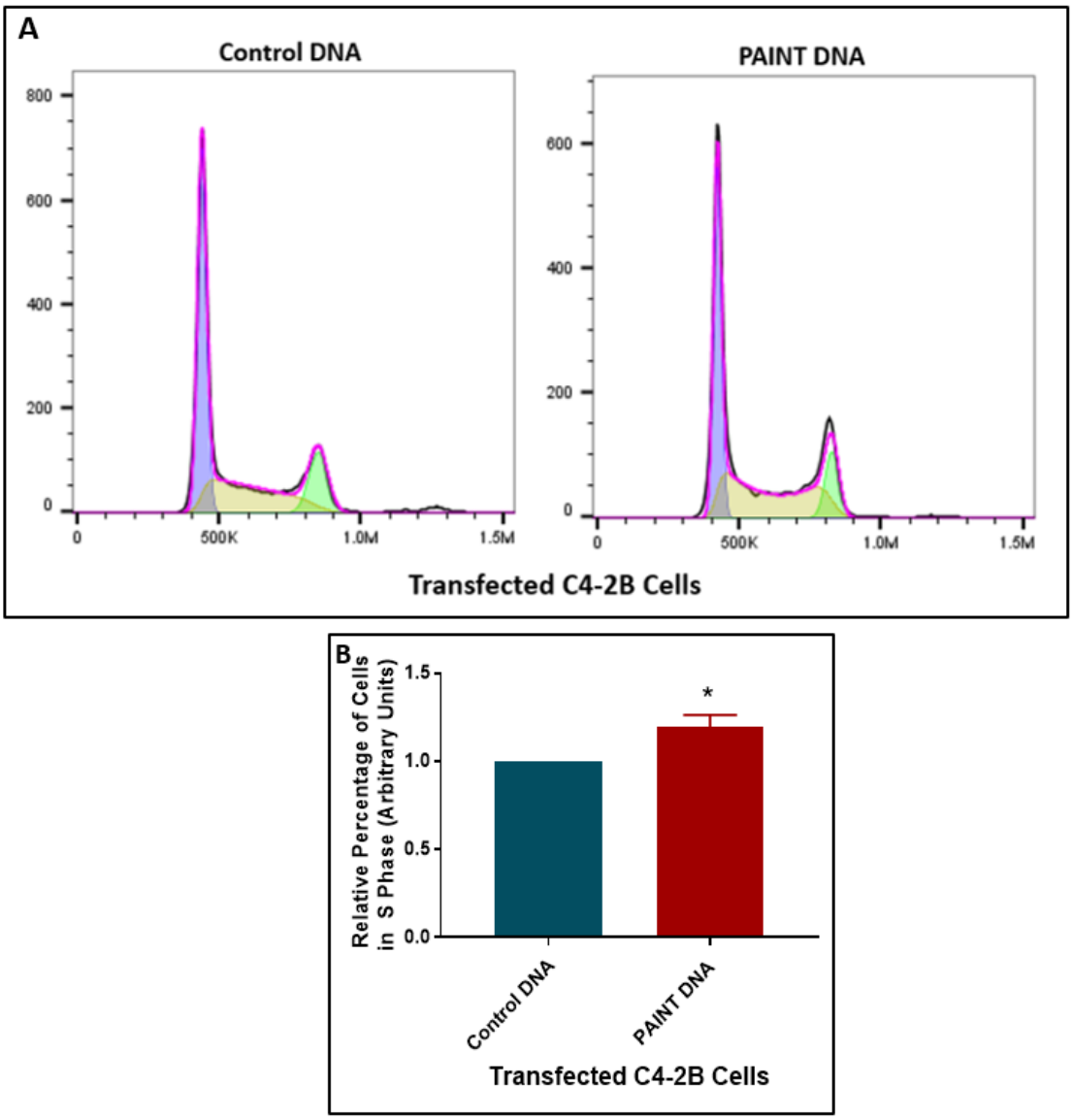

Figure 20: Overexpression of PAINT enhanced cell cycle progression of C4-2B cells.

(A) Two parameter histogram of cell cycle progression of PI stained C4-2B cells stably transfected with pcDNA-control (left) and pcDNA-PAINT (right). (B) Comparative analysis of percentage of cells in S phase showing an increase (19%) in S phase population of C4-2B cells stably expressing pcDNA-PAINT compared to pcDNA-control C4-2B subline. Data show the mean ± SD for 3 biological replicates. *p = 0.036.

4.2.2.3 Overexpression of PAINT Promotes Larger Colony Formation and Expression of Ki-67 Proliferation Marker

In this study, we examined the effect of PAINT expression in colony formation. We used soft agar colony formation assay using stably transfected sublines of C4-2B cells. Our results showed that overexpression of PAINT promoted formation of higher percentage of larger colonies compared to control C4-2B cells (Figure 21A and 21B). This observation suggests that PAINT expression promotes tumorigenicity in C4-2B cells.

Furthermore, we examined proportion of actively proliferating cells by Ki-67 staining using immunofluorescence assay of stably transfected C4-2B sublines. C4-2B cells overexpressing PAINT showed higher percentage of Ki-67 positive cells compared to control C4-2B subline. This observation indicates that PAINT positively regulate cell proliferation of C4-2B cells.

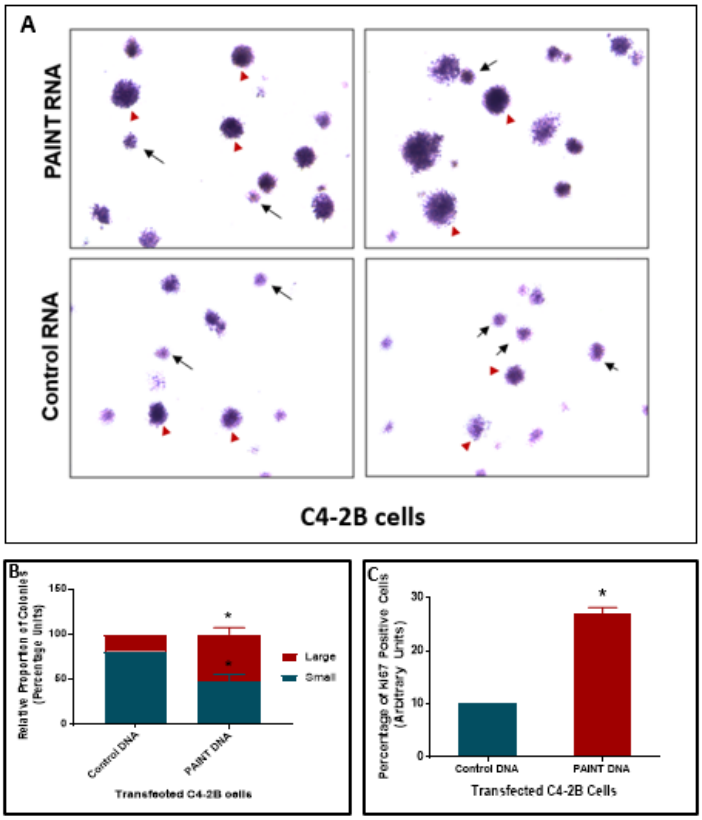

Figure 21: Overexpression of PAINT promoted larger colony formation and increased expression of Ki-67

(A) Representative images of soft agar colonies formed by C4-2B subline overexpressing PAINT (top images) and control subline (bottom images). Red arrows represented large colonies and small black arrows represented small colonies (B) Quantitative analysis of the number of small (<7 µm) and large (>7 µm) of colonies showing that C4-2B cells overexpressing PAINT formed more (52%) large colonies compared to C4-2B control subline (19%). Data show the mean ± SD of 3 biological replicates. *p < 0.0001. (C) Enumeration of Ki-67 positive cells showing higher percentage of Ki-67 positive cells (27%) in C4-2B subline overexpressing PAINT than control C4-2B subline (10.28%). Data show the mean ± SD. *p = 0.03.

4.2.2.4 Overexpression of PAINT Enhances Cell Migration and Expression of Mesenchymal Marker Slug.

Overexpression of PAINT increased cell proliferation, promoted S phase progression and facilitated larger colony formation. In this experiment, we determined the functional association of PAINT in migratory properties of C4-2B cells. Overexpression of PAINT showed 34% higher rate of cell migration compared to C4-2B control cells (Figure 22A and 22B). These results show a positive effect of PAINT expression on cell migration of prostate cancer cells.

To confirm that the pro-migratory effects of PAINT is mediated through alteration of expression of EMT markers we performed Western blot analysis. Our analysis showed that overexpression of PAINT increased expression Slug (96%) (Figure 23A and 23B) and decreased expression of E-Cadherin (13%) (Figure 23A and 23C). Altogether, our results indicate that overexpression of PAINT promotes cell migration and modulate expression of EMT markers.

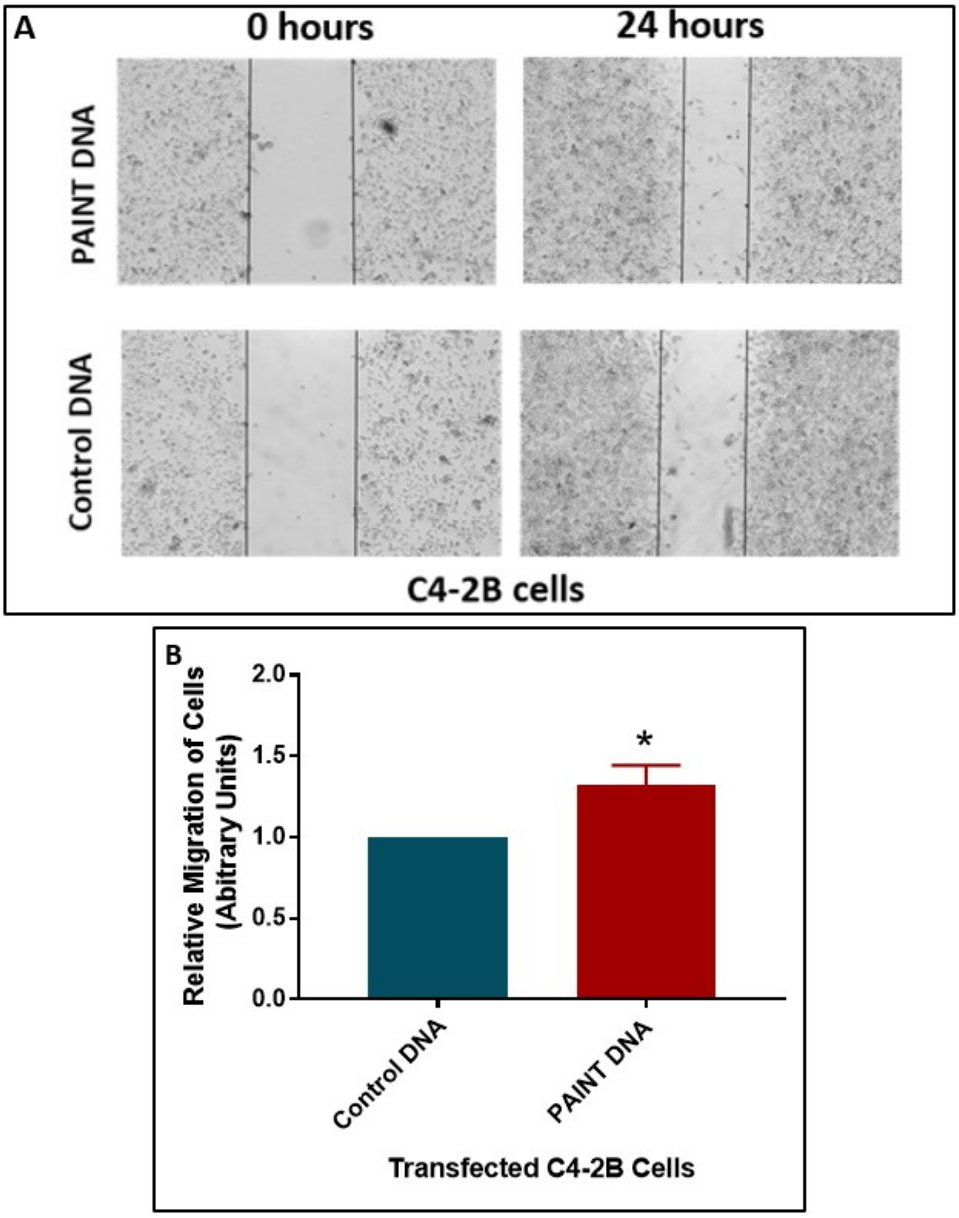

Figure 22: Overexpression of PAINT increases cell migration

(A) Representative images of cell migration of C4-2B cells overexpressing PAINT (top) and C4-2B control cells (bottom) at 0 hours (left) and 24 hours (right) after making the scratch. (B) Analysis of the rate of migration showing increased cell migration (34%) of C4-2B cells over-expressing PAINT compared to control cell lines. Data were represented as mean ± SD for 3 biological replicates. *$p = 0.01$.

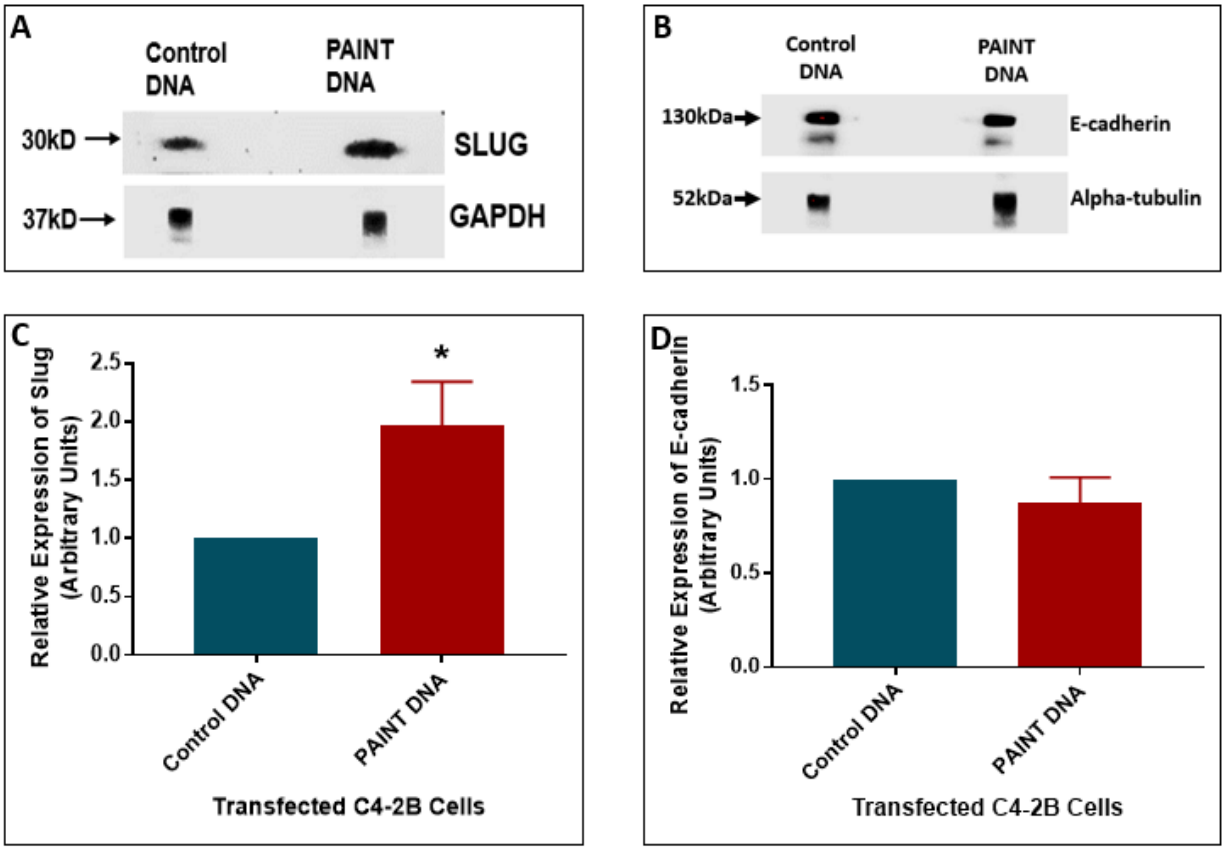

Figure 23: Overexpression of PAINT increased expression of mesenchymal marker Slug and decreased epithelial marker E-cadherin.

(A, B) Representative Western blot images showing expression of Slug (left) and E-cadherin (right) in C4-2B cell lysates. Overexpression of PAINT in C4-2B cells increased expression of Slug and decreased expression of E-cadherin compared to control C4-2B subline. (C) Densitometry of Slug and E-cadherin expression in C4-2B cells transfected with PAINT DNA or Control DNA. Overexpression of PAINT increased Slug expression by 96% and reduced E-cadherin expression by 13%. Data show the mean ± SD of three biological replicates. *p= 0.047.

CHAPTER FIVE: DISCUSSION

Previous studies in our lab established that miR-17-92a microRNA cluster was down-regulated in prostate tumors and prostate cancer cell lines and exhibited an overall tumor suppressor function in prostate cancer. Transcriptome profiling study in our lab showed dysregulation of many protein coding transcripts as well as non-coding transcripts, including lncRNAs in miR-17-92a expressing PC-3 cells. Emerging evidences from recent studies demonstrated that aberrantly expressed lncRNAs may play significant roles in the progression of prostate cancer (83). Our study mainly focused on characterizing the function of dysregulated lncRNAs in prostate cancer. We specifically searched for lncRNAs that were downregulated as a result of overexpression of miR-17-92a miRNA cluster. We also restricted our search to intergenic lncRNAs that were altered. We selected top three candidates based on their intergenic positions, >2-fold differential expression and expression cut-off value at 20 FPKM. In silico expression analysis based on NONCODE, UCSC Genome Browser, EMBL expression atlas, NCBI GEO profiles, and published studies on selected lncRNAs in cancer revealed that one of the selected lncRNAs, PAINT, is overexpressed in several other cancers including metastatic esophageal squamous cell cancer (97) (98), melanoma (99), colon cancer (100) and lung cancer (101). Previous studies also showed that androgen deprivation therapy increased expression of PAINT in prostate cancer cells (102). Furthermore, distant metastatic prostate cancer cell lines aberrantly expressed PAINT compared to other prostate cancer and non-tumorigenic prostate cell lines. Previous RNA sequencing-based studies revealed that distant metastatic VCaP and PC-3 cells show 3-fold higher expression of PAINT compared to the less aggressive cell lines such as LNCaP and 22Rv1 and normal prostate cell line RWPE-1

(95). Our study using qRT-PCR analysis found 8 to 10-fold higher expression of PAINT in PC-3 cells compared to the less aggressive C4-2B, LNCaP-104S, 22Rv1 cells and RWPE-1 normal prostate cell line. Our study on TMA expression analysis using RNA-ISH showed upregulation of PAINT in prostate cancer tissues in comparison with normal prostate tissues. Furthermore, comparative analysis of expression in different stages of prostate cancer showed higher expression of PAINT in stage III and stage IV compared to stage II prostate cancer patient tissues. Taken together, aberrant expression of PAINT in prostate cancer, especially in the late stage and castration resistant prostate cancer (as noted in database analysis) (102) (96), suggests that PAINT may have potential oncogenic functions and possibly acts as a driver oncogene to promote development and progression of aggressive prostate cancer.

Our studies on functional analysis showed that silencing of PAINT altered tumor phenotypes of the highly aggressive PC-3 cells. These phenomena were noted through altered cell morphology, reduced cell proliferation (26%) and decreased S phase cell population (26%). Importantly, our studies on overexpression of PAINT in less aggressive and androgen sensitive C4-2B cells reversed the effects noted in the silencing experiments. Overexpression of PAINT increased C4-2B cell proliferation (52%) and increased S phase cell population (19%). Additionally, overexpression of PAINT promoted larger colony formation (53% large colonies) compared to control C4-2B cells (19% large colonies). These observations indicate that up regulation of PAINT as noted in advanced stage prostate cancer may contribute to cancer progression by enhancing proliferation potential of prostate cancer cells.

Our study also demonstrated that PAINT expression may contribute to prostate cancer cell survival as silencing of PAINT activated pro-apoptotic proteins, PARP and Caspase-3. Caspase-3 and PARP are two major proteins involved in the apoptotic pathways and play critical roles in induction of apoptosis (103) (104). These observations suggest that PAINT expression facilitates cell growth and tumorigenicity by regulating cell cycle progression and apoptosis in highly metastatic PC-3 prostate cancer cell line.

Another hallmark of aggressive cancer is increased cell migration. Our study further showed that PAINT is involved in promoting EMT. Results of our study showed that silencing of PAINT reduced migration of PC-3 cells (33%) compared to control PC-3 cells. In contrast, ectopic expression of PAINT increased migration of C4-2B cells (34%). Additionally, protein expression analysis showed that mesenchymal markers Slug and Vimentin were downregulated (57% and 87% respectively), and the epithelial marker E-cadherin was upregulated (39%) upon silencing of PAINT in PC-3 cells. A reverse effect was noted upon overexpression of PAINT, which showed a significantly higher expression of Slug (97%) and decreased expression of E-cadherin (13%). Slug is one of the major transcription factors which induces epithelial mesenchymal transition (105) and promotes prostate cancer cell migration and invasion (106). It is well documented that Vimentin overexpression promotes prostate cancer invasion and metastasis and is commonly regulated by Slug (107) (108). Furthermore, Slug directly inhibits E-cadherin expression and downregulation of E-cadherin promotes metastasis of prostate cancer (109). All these observations indicate that PAINT may regulate migration and invasive properties of highly metastatic PC-3 prostate cancer cells by regulating the expression of Slug, Vimentin and E-cadherin. Taken together, both silencing and overexpression studies strongly indicate that PAINT plays an essential

role in cancer cell migration and may contribute to cancer metastasis. Our study demonstrated that silencing of PAINT had antiproliferative and antimigratory effects, which suggest that silencing of PAINT may have therapeutic benefit in combination therapy for improving drug sensitivity. Our drug sensitivity assays showed that silencing of PAINT significantly improved the sensitivity of DTX (20% less viability), a commonly used chemotherapeutic agent, to PC-3 cells. DTX prevents microtubule dynamic assembly and disassembly and inhibits mitotic cell division in the metaphase and anaphase eventually inducing apoptosis (110). Our results on the drug sensitivity assays suggest that activation of apoptotic pathways may have a synergistic effect with DTX treatments, and this combination therapy could be used as a promising therapeutic approach to treat metastatic prostate cancer in future.

5.1 Conclusion and Future Directions

Our studies based on TMA analysis of prostate cancer specimens and functional characterization strongly suggest that aberrantly expressed PAINT lncRNA may function as a cancer driver and contribute to prostate cancer progression by enhancing proliferation, cell cycle progression and cell survival. Our studies also suggest that PAINT may enhance metastatic potential by promoting cell migration through regulating metastasis markers Slug, Vimentin and E-cadherin. However, it is not clear how PAINT modulates these events and promotes cancer progression. Our initial finding provides the foundation for exploring the underlying mechanism by which PAINT play regulatory roles in prostate cancer progression and metastasis. Whole genome transcription profiling may provide valuable insights about the functional role of PAINT in modulating the transcriptional landscape of prostate cancer cells and their involvement in different pathways and cancer related features. To find out the molecular basis of PAINT function in prostate cancer, we

need to identify its interacting partners which could be proteins, RNAs and DNAs. Our ongoing studies based on RNA immunoprecipitation and mass spectrometry showed that PAINT interacts with several important proteins involved in translation initiation, mRNA metabolism and transport, and prostate cancer (data were not presented). This information opens new areas for further investigation of PAINT function. Additionally, xenograft studies may provide valuable insights about its functional role in prostate cancer progression and metastasis.

REFERENCES

1. Berretta J, Morillon A. Pervasive transcription constitutes a new level of eukaryotic genome regulation. EMBO Rep. 2009;10(9):973–82.

2. Cech TR, Steitz JA. The noncoding RNA revolution - Trashing old rules to forge new ones. Cell. 2014;157(1):77–94.

3. Esteller M. Non-coding RNAs in human disease. Nat Rev Genet. 2011;12(12):861–74.

4. Anastasiadou E, Jacob LS, Slack FJ. Non-coding RNA networks in cancer. Nat Rev Cancer. 2017 Nov 24; 18:5.

5. Rinn JL, Chang HY. Genome regulation by long noncoding RNAs. Annu Rev Biochem

6. Gascoigne DK, Cheetham SW, Cattenoz PB, Clark MB, Amaral PP, Taft RJ, et al. Pinstripe: A suite of programs for integrating transcriptomic and proteomic datasets identifies novel proteins and improves differe. Bioinformatics. 2012;28(23):3042–50.

7. Guttman M, Amit I, Garber M, French C, Lin MF, Feldser D, et al. Chromatin signature reveals over a thousand highly conserved large non-coding RNAs in mammals. Nature

8. Quinn JJ, Chang HY. Unique features of long non-coding RNA biogenesis and function. Nat Rev Genet. 2015;17(1):47–62.

9. Derrien T, Johnson R, Bussotti G, Tanzer A, Djebali S, Tilgner H, et al. The GENCODE v7 catalogue of human long non-coding RNAs: Analysis of their structure, evolution and expression. Genome Res. 2012; 22:1775–89.

10. Cabili M, Trapnell C, Goff L, Koziol M, Tazon-Vega B, Regev A, et al. Integrative annotation of human large intergenic noncoding RNAs reveals global properties and specific subclasses. Genes Dev. 2011;25(18):1915–27.

11. Carninci P, Kasukawa T, Katayama S, Gough J, Frith MC, Maeda N, et al. Molecular biology: The transcriptional landscape of the mammalian genome. Science (80-). 2005;309(5740):1559–63.

12. Tang Q, Hu G, Escobar TM, Zhu J, Zhao K, Sharma S, et al. Expression and regulation of intergenic long noncoding RNAs during T cell development and differentiation. Nat Immunol. 2013;14(11):1190–8.

13. Amaral PP, Mattick JS. Noncoding RNA in development. Mammalian Genome. 2008;19(7–8):454–92.

14. Brunner AL, Beck AH, Edris B, Sweeney RT, Zhu SX, Li R, et al. Transcriptional profiling of long non-coding RNAs and novel transcribed regions across a diverse panel of archived human cancers. Genome Biol. 2012;13(8): R75.

15. Zheng GXY, Do BT, Webster DE, Khavari P a, Chang HY. Dicer-microRNA-Myc circuit promotes transcription of hundreds of long noncoding RNAs. Nat Struct Mol Biol. 2014;21(7):585–90.

16. Gupta S, Sigova AA, Molinie B, Lin C, Giallourakis CC, Almada AE, et al. Divergent transcription of long noncoding RNA/mRNA gene pairs in embryonic stem cells. Proc Natl Acad Sci. 2013;110(8):2876–81.

17. Rahl PB, Yeo GW, Calabrese JM, Young RA, Levine SS, Flynn RA, et al. Divergent Transcription from Active Promoters. Science (80-). 2008;322(5909):1849–51.

18. Almada AE, Wu X, Kriz AJ, Burge CB, Sharp PA. Promoter directionality is controlled by U1 snRNP and polyadenylation signals. Nature. 2013 Jun 23; 499:360.

19. Wilusz JE. Long noncoding RNAs: Re-writing dogmas of RNA processing and stability. Biochim Biophys Acta - Gene Regul Mech. 2016;1859(1):128–38.

20. Wilusz JE, Freier SM, Spector DL. 3′ End Processing of a Long Nuclear-Retained Noncoding RNA Yields a tRNA-like Cytoplasmic RNA. Cell. 2008;135(5):919–32.

21. Rajnish A. Gupta, Nilay Shah, Kevin C. Wang, Jeewon Kim, Hugo M. Horlings DJ, Wong, Miao-Chih Tsai, Tiffany Hung, Pedram Argani, John L. Rinn, Yulei Wang P, Brzoska, Benjamin Kong, Rui Li, Robert B. West, Marc J. van de Vijver S, Sukumar and HYC. Long noncoding RNA HOTAIR reprograms chromatin state to promote cancer metastasis. Nature. 2010;

22. Clemson CM, Hutchinson JN, Sara SA, Ensminger AW, Fox AH, Chess A, et al. An Architectural Role for a Nuclear Noncoding RNA: NEAT1 RNA Is Essential for the Structure of Paraspeckles. Mol Cell. 2009 Mar 27;33(6):717–26.

23. Yu Y, Zhang M, Liu J, Xu B, Yang J, Wang N, et al. Long Non-coding RNA PVT1 Promotes Cell Proliferation and Migration by Silencing ANGPTL4 Expression in Cholangiocarcinoma. Mol Ther - Nucleic Acids. 2018 Dec 7; 13:503–13.

24. Tripathi V, Ellis JD, Shen Z, Song DY, Pan Q, Watt AT, et al. The Nuclear-Retained Noncoding RNA MALAT1 Regulates Alternative Splicing by Modulating SR Splicing Factor Phosphorylation. Mol Cell. 2010;39(6):925–38.

25. Chen L-L. Linking Long Noncoding RNA Localization and Function. Trends Biochem Sci. 2016;41(9):761–72.

26. Lubelsky Y, Ulitsky I, Tichon A, Havkin Solomon T, Itzkovitz S, Lemze D, et al. A conserved abundant cytoplasmic long noncoding RNA modulates repression by Pumilio proteins in human cells. Nat Commun. 2016;7(1):1–10.

27. Yoon JH, Abdelmohsen K, Srikantan S, Yang X, Martindale JL, De S, et al. LincRNA-p21 Suppresses Target mRNA Translation. Mol Cell. 2012;47(4):648–55.

28. Liu B, Sun L, Liu Q, Gong C, Yao Y, Lv X, et al. A Cytoplasmic NF-κ B Interacting Long Noncoding RNA Blocks Iκ B Phosphorylation and Suppresses Breast Cancer Metastasis. Cancer Cell. 2015 Mar 9;27(3):370–81.

29. Essers PB, van Heesch S, Boymans S, de Bruijn E, Cuppen E, van Iterson M, et al. Extensive localization of long noncoding RNAs to the cytosol and mono- and polyribosomal complexes. Genome Biol. 2014;15(1): R6.

30. Bartel DP. MicroRNAs: Target Recognition and Regulatory Functions. Cell. 2009 Jan 23;136(2):215–33.

31. MacFarlane L-A, R. Murphy P. MicroRNA: Biogenesis, Function and Role in Cancer. Curr Genomics. 2010;11(7):537–61.

32. Ha M, Kim VN. Regulation of microRNA biogenesis. Nat Rev Mol Cell Biol. 2014 Jul 16; 15:509.

33. Institute N cancer. Prostate cancer-patient version: overview.

34. Siegel RL, Miller KD, Jemal A. Cancer Statistics, 2018. CA Cancer J Clin. 2018; 68:7–30.

35. American Cancer Society: Cancer Facts and Figures 2019. Atlanta, Ga: American Cancer Society, 2019.

36. Society AC. Prostate cancer stages.

37. Chan TY, Partin AW, Walsh PC, Epstein JI. Prognostic significance of Gleason score 3+4 versus Gleason score 4+3 tumor at radical prostatectomy. Urology In. 2000 Nov 1;56(5):823–7.

38. Society AC. Treating prostate cancer: watchful waiting or active surveillance of prostate cancer.

39. Feldman BJ, Feldman D. The development of androgen-independent prostate cancer. Nat Rev Cancer. 2001;1(1):34–45.

40. Karantanos T, Corn PG, Thompson TC. Prostate cancer progression after androgen deprivation therapy: Mechanisms of castrate resistance and novel therapeutic approaches. Oncogene

41. Culig Z, Hobisch A, Cronauer MV, Radmayr C, Trapman J, Hittmair A, et al. Androgen receptor activation in prostatic tumor cell lines by insulin-like growth factor-1, keratinocyte growth factor and epidermal growth factor. Cancer Res. 1994;54(20):5474–8.

42. Stanbrough M, Bubley GJ, Ross K, Golub TR, Rubin MA, Penning TM, et al. Increased expression of genes converting adrenal androgens to testosterone in androgen-independent prostate cancer. Cancer Res. 2006;66(5):2815–25.

43. Gutschner T, Diederichs S. The hallmarks of cancer: A long non-coding RNA point of view. RNA Biol. 2012;9(6):703–9.

44. Arun G, Diermeier SD, Spector DL. Therapeutic Targeting of Long Non-Coding RNAs in Cancer. Trends Mol Me. 2018;24(3):257–77.

45. Huarte M, Guttman M, Feldser D, Garber M, Koziol MJ, Kenzelmann-Broz D, et al. A large intergenic noncoding RNA induced by p53 mediates global gene repression in the p53 response. Cell. 2010;142(3):409–19.

46. Dugimont T, Montpellier C, Adriaenssens E, Lottin S, Dumont L, Iotsova V, et al. The H19 TATA-less promoter is efficiently repressed by wild-type tumor suppressor gene product p53. Oncogene. 1998;16(18):2395–401.

47. Berteaux N, Lottin S, Monté D, Pinte S, Quatannens B, Coll J, et al. H19 mRNA-like noncoding RNA promotes breast cancer cell proliferation through positive control by E2F1. J Biol Chem. 2005;280(33):29625–36.

48. Zhang A, Zhao JC, Kim J, Fong K wing, Yang YA, Chakravarti D, et al. LncRNA HOTAIR Enhances the Androgen-Receptor-Mediated Transcriptional Program and Drives Castration-Resistant Prostate Cancer. Cell Rep. 2015;13(1):209–21.

49. Gutschner T, Hämmerle M, Eißmann M, Hsu J, Kim Y, Hung G, et al. The noncoding RNA MALAT1 is a critical regulator of the metastasis phenotype of lung cancer cells. Cancer Res. 2013;73(3):1180–9.

50. Tripathi V, Shen Z, Chakraborty A, Giri S, Freier SM, Wu X, et al. Long Noncoding RNA MALAT1 Controls Cell Cycle Progression by Regulating the Expression of Oncogenic Transcription Factor B-MYB. PLoS Genet. 2013;9(3).

51. Hudson WH, Pickard MR, De Vera IMS, Kuiper EG, Mourtada-Maarabouni M, Conn GL, et al. Conserved sequence-specific lincRNA-steroid receptor interactions drive transcriptional repression and direct cell fate. Nat Commun. 2014; 5:1–13.

52. Pickard MR, Williams GT. Molecular and cellular mechanisms of action of tumour suppressor GAS5 LncRNA. Genes (Basel). 2015;6(3):484–99.

53. Gil J, Peters G. Regulation of the INK4b–ARF–INK4a tumor suppressor locus: all for one or one for all. Nat Rev Mol Cell Biol. 2006 Sep 1; 7:667.

54. Marín-Béjar O, Marchese FP, Athie A, Sánchez Y, González J, Segura V, et al. Pint lincrna connects the p53 pathway with epigenetic silencing by the polycomb repressive complex 2. Genome Biol. 2013;14(9).

55. Sauvageau M, Sauvageau G. Polycomb group proteins: Multi-faceted regulators of somatic stem cells and cancer. Cell Stem Cell. 2010;7(3):299–313.

56. Srikantan V, Zou Z, Petrovics G, Xu L, Augustus M, Davis L, et al. PCGEM1, a prostate-specific gene, is overexpressed in prostate cancer. Proc Natl Acad Sci. 2000;97(22):12216–21.

57. J.-H. H, J.-Z. Z, Z.-P. H, L. W, Y.B. L, Y.-G. L. Reciprocal regulation of PCGEM1 and miR-145 promote proliferation of LNCaP prostate cancer cells. J Exp Clin Cancer Res. 2014;33(1):1–10.

58. Prensner JR, Iyer MK, Sahu A, Asangani IA, Cao Q, Patel L, et al. The long noncoding RNA SChLAP1 promotes aggressive prostate cancer and antagonizes the SWI/SNF complex. Nat Genet. 2013 Sep 29; 45:1392.

59. Wang Z, Wang S, Duan J, Xiao N, Li Y, Luo H. Long Noncoding RNA SChLAP1 Accelerates the Proliferation and Metastasis of Prostate Cancer via Targeting miR-198 and Promoting the MAPK1 Pathway. Oncol Res Featur Preclin Clin Cancer Ther. 2017;26(1):131–43.

60. Wang L, Xiao X, Wu X, Jiang G, Tao D, Zeng F, et al. Long Non-Coding RNA MEG3 Inhibits Cell Proliferation and Induces Apoptosis in Prostate Cancer. Cell Physiol Biochem. 2015;37(6):2209–20.

61. Wang X, Ruan Y, Wang X, Zhao W, Jiang Q, Jiang C, et al. Long intragenic non-coding RNA lincRNA-p21 suppresses development of human prostate cancer. Cell Prolif. 2017;50(2):1–10.

62. Huarte M. The emerging role of lncRNAs in cancer. Nat Med . 2015 Nov;21(11):1253–61.

63. Vickers TA, Koo S, Bennett CF, Crooke ST, Dean NM, Baker BF. Efficient reduction of target RNAs by small interfering RNA and RNase H-dependent antisense agents. A comparative analysis. J Biol Chem. 2003;278(9):7108–18.

64. Ren S, Liu Y, Xu W, Sun Y, Lu J, Wang F, et al. Long noncoding RNA MALAT-1 is a new potential therapeutic target for castration resistant prostate cancer. J Urol. 2013;190(6):2278–87.

65. Dowdy SF. Overcoming cellular barriers for RNA therapeutics. Nat Biotechnol. 2017 Feb 27; 35:222.

66. Dias N, Stein CA. Antisense oligonucleotides: basic concepts and mechanisms. Mol Cancer Ther. 2002;1(5):347–55.

67. Bennett CF, Baker BF, Pham N, Swayze E, Geary RS. Pharmacology of Antisense Drugs. Annu Rev Pharmacol Toxicol. 2017 Jan 6;57(1):81–105.

68. Parsons C, Slack FJ, Zhang WC, Adams BD, Walker L. Targeting noncoding RNAs in disease. J Clin Invest. 2017;127(3):761–71.

69. Lima W, Wu H, Crooke ST. The RNase H mechanism. In: Antisense Drug Technology: Principles, Strategies, and Applications, Second Edition. 2007. p. 47–74.

70. Bergmann JH, Spector DL. Long non-coding RNAs: Modulators of nuclear structure and function. Curr Opin Cell Biol. 2014;26(1):10–8.

71. Bassik MC, Chen Y, Qi LS, Weissman JS, Panning B, Ploegh HL, et al. Genome-Scale CRISPR-Mediated Control of Gene Repression and Activation. Cell. 2014;159(3):647–61.

72. Tseng Y-Y, Moriarity BS, Gong W, Akiyama R, Tiwari A, Kawakami H, et al. PVT1 dependence in cancer with MYC copy-number increase. Nature. 2014 Jun 22; 512:82.

73. Trimarchi T, Bilal E, Ntziachristos P, Fabbri G, Dalla-Favera R, Tsirigos A, et al. Genome-wide Mapping and Characterization of Notch-Regulated Long Noncoding RNAs in Acute Leukemia. Cell. 2014 Jul 31;158(3):593–606.

74. Katayama S, Tomaru Y, Kasukawa T, Waki K, Nakanishi M, Nakamura M, et al. Antisense Transcription in the Mammalian Transcriptome. Science (80-). 2005 Sep 2;309(5740):1564 LP-1566.

75. Faghihi MA, Wahlestedt C. Regulatory roles of natural antisense transcripts. Nat Rev Mol Cell Biol. 2009 Jul 29; 10:637.

76. Modarresi F, Faghihi MA, Lopez-Toledano MA, Fatemi RP, Magistri M, Brothers SP, et al. Inhibition of natural antisense transcripts in vivo results in gene-specific transcriptional upregulation. Nat Biotechnol. 2012 Mar 25; 30:453.

77. Zhou M-M, Walsh MJ, Yap KL, Raguz S, Li S, Zeng L, et al. Molecular Interplay of the Noncoding RNA ANRIL and Methylated Histone H3 Lysine 27 by Polycomb CBX7 in Transcriptional Silencing of INK4a. Mol Cell. 2010;38(5):662–74.

78. Jong RM, Soukup D, Jacks T, Lee JT, Dimitrova N, Sharp PA, et al. LincRNA-p21 Activates p21 in cis to Promote Polycomb Target Gene Expression and to Enforce the G1/S Checkpoint. Mol Cell. 2014;54(5):777–90.

79. D. A, A. H. Development of targeted therapy for bladder cancer mediated by a double promoter plasmid expressing diphtheria toxin under the control of H19 and IGF2-P4 regulatory sequences. J Transl Med. 2010; 8:1–18.

80. Sidi AA, Ohana P, Benjamin S, Shalev M, Ransom JH, Lamm D, et al. Phase I/II marker lesion study of intravesical BC-819 DNA plasmid in H19 over expressing superficial bladder cancer refractory to bacillus Calmette-Guerin. J Urol. 2008;180(6):2379–83.

81. Rivas E, Clements J, Eddy SR. A statistical test for conserved RNA structure shows lack of evidence for structure in lncRNAs. Nat Methods. 2017;14(1):45.

82. Wilusz JE, JnBaptiste CK, Lu LY, Kuhn CD, Joshua-Tor L, Sharp PA. A triple helix stabilizes the 3′ ends of long noncoding RNAs that lack poly(A) tails. Genes Dev. 2012;26(21):2392–407.

83. Melo SA, Esteller M. Dysregulation of microRNAs in cancer: Playing with fire. FEBS Lett. 2011;585(13):2087–99.

84. Sood P, Krek A, Zavolan M, Macino G, Rajewsky N. Cell-type-specific signatures of microRNAs on target mRNA expression. Proc Natl Acad Sci. 2006.

85. Dalmay T, Edwards DR. MicroRNAs and the hallmarks of cancer. Oncogene. 2006;25(46):6170–5.

86. Hayes J, Peruzzi PP, Lawler S. MicroRNAs in cancer: biomarkers, functions and therapy. Trends Mol Med. 2014 Aug 1;20(8):460–9.

87. Cavaliere C, Veneziani BM, Montanari M, Stiuso P, Pepe MF, Quagliuolo L, et al. Micrornas in prostate cancer: an overview. Oncotarget. 2017;8(30):50240–51.

88. Gibbons DL, Lin W, Creighton CJ, Rizvi ZH, Gregory PA, Goodall GJ, et al. Contextual extracellular cues promote tumor cell EMT and metastasis by regulating miR-200 family expression. Genes Dev. 2009;23(18):2140–51.

89. Sun X, Liu J, Xu C, Tang SC, Ren H. The insights of Let-7 miRNAs in oncogenesis and stem cell potency. J Cell Mol Med. 2016;20(9):1779–88.

90. Mo W, Zhang J, Li X, Meng D, Gao Y, Yang S, et al. Identification of Novel AR-Targeted MicroRNAs Mediating Androgen Signalling through Critical Pathways to Regulate Cell Viability in Prostate Cancer. PLoS One. 2013;8(2).

91. Nicorici D, Kohonen P, Kangaspeska S, Ostling P, Leivonen S-K, Perala M, et al. Systematic Analysis of MicroRNAs Targeting the Androgen Receptor in Prostate Cancer Cells. Cancer Res. 2011;71(5):1956–67.

92. Zhao J, Wang Z-Y, Eischeid AN, Young CY, Chen D, Gong A-Y, et al. miR-17-5p targets the p300/CBP-associated factor and modulates androgen receptor transcriptional activity in cultured prostate cancer cells. BMC Cancer. 2012;12(1).

93. Ottman R, Levy J, Williams GE, Chakrabarti R. The other face of miR-17-92a cluster, exhibiting tumor suppressor effects in prostate cancer. Oncotarget. 2016;7(45):73739–53.

94. Cunningham D, You Z. In vitro and in vivo model systems used in prostate cancer research. J Biol Methods. 2015;2(1):17.

95. Barretina J, Caponigro G, Stransky N, Venkatesan K, Margolin AA, Kim S, et al. The Cancer Cell Line Encyclopedia enables predictive modelling of anticancer drug sensitivity. Nature [Internet]. 2012 Mar 28; 483:603.

96. D'Antonio JM, Ma C, Monzon FA, Pflug BR. Longitudinal analysis of androgen deprivation of prostate cancer cells identifies pathways to androgen independence. Prostate. 2008 May 15;68(7):698–714.

97. Qin H De, Liao XY, Chen Y Bin, Huang SY, Xue WQ, Li FF, et al. Genomic Characterization of Esophageal Squamous Cell Carcinoma Reveals Critical Genes Underlying Tumorigenesis and Poor Prognosis. Am J Hum Genet. 2016;98(4):709–27.

98. Tong M, Chan KW, Bao JYJ, Wong KY, Chen JN, Kwan PS, et al. Rab25 is a tumor suppressor gene with antiangiogenic and anti-invasive activities in esophageal squamous cell carcinoma. Cancer Res. 2012;72(22):6024–35.

99. Wang S, Fan W, Wan B, Tu M, Jin F, Liu F, et al. Characterization of long noncoding RNA and messenger RNA signatures in melanoma tumorigenesis and metastasis. PLoS One. 2017;12(2):1–20.

100. Tanaka H, Uetake H, Yoshida T, Mizushima H, Matsuyama T, Mogushi K, et al. MUC12 mRNA expression is an independent marker of prognosis in stage II and stage III colorectal cancer. Int J Cancer. 2010;127(10):2292–9.

101. Liu B, Chen Y, Yang J. LncRNAs are altered in lung squamous cell carcinoma and lung adenocarcinoma. Oncotarget. 2016;8(15):24275–91.

102. Wang Q, Li W, Liu XS, Carroll JS, Jänne OA, Keeton EK, et al. A Hierarchical Network of Transcription Factors Governs Androgen Receptor-Dependent Prostate Cancer Growth. Mol Cell. 2007 Aug 3;27(3):380–92.

103. Boulares AH, Yakovlev AG, Ivanova V, Stoica BA, Wang G, Iyer S, et al. Role of Poly (ADP-ribose) Polymerase (PARP) Cleavage in Apoptosis. 1999;274(33):22932–40.

104. Wong RSY. Apoptosis in cancer: From pathogenesis to treatment. J Exp Clin Cancer Res . 2011;30(1):87.

105. Medici D, Hay ED, Olsen BR. Snail and Slug promote epithelial-mesenchymal transition through β-catenin–T-cell factor-4-dependent expression of transforming growth factor-β3. Mol Biol Cell. 2008;19(11):4875–87.

106. Uygur B, Wu WS. SLUG promotes prostate cancer cell migration and invasion via CXCR4/CXCL12 axis. Mol Cancer. 2011;10(1):139.

107. Wei J, Xu G, Wu M, Zhang Y, Li Q, Liu P, et al. Overexpression of vimentin contributes to prostate cancer invasion and metastasis via Src regulation. Anticancer Res. 2008;28(1 A):327–34.

108. Singh S, Sadacharan S, Su S, Belldegrun A, Persad S, Singh G. Overexpression of vimentin: Role in the invasive phenotype in an androgen-independent model of prostate cancer. Cancer Res. 2003;63(9):2306–11.

109. Putzke AP, Ventura AP, Bailey AM, Akture C, Opoku-Ansah J, Çeliktaş M, et al. Metastatic progression of prostate cancer and E-cadherin: Regulation by ZEB1 and Src family kinases. Am J Pathol. 2011;179(1):400–10.

110. Yvon AM, Wadsworth P, Jordan MA. Taxol suppresses dynamics of individual microtubules in living human tumor cells. Mol Biol Cell. 1999;10(4):947–59.